

**RECOVERY AND SEPARATION OF CELLULOSE FROM SAWDUST  
WOOD HYDROLYSATES USING MEMBRANE REACTOR: EFFECT OF  
TRANSMEMBRANE PRESSURE (TMP) AND CROSS FLOW VELOCITY  
(CFV)**

**MOHAMAD AFIS BIN ADNAN**

**UNIVERSITI MALAYSIA PAHANG**

# UNIVERSITI MALAYSIA PAHANG

## BORANG PENGESAHAN STATUS TESIS

JUDUL: **RECOVERY AND SEPARATION OF CELLULOSE FROM SAWDUST  
WOOD HYDROLYSATES USING MEMBRANE REACTOR: EFFECT  
OF TRANSMEMBRANE PRESSURE (TMP) AND CROSS FLOW  
VELOCITY (CFV)**

SESI PENGAJIAN: **2010/2011**

Saya **MOHAMAD AFIS BIN ADNAN**  
(HURUF BESAR)

mengaku membenarkan tesis Projek Sarjana Muda (PSM) ini disimpan di Perpustakaan Universiti Malaysia Pahang dengan syarat-syarat kegunaan seperti berikut:

1. Hakmilik kertas projek adalah di bawah nama penulis melainkan penulisan sebagai projek bersama dan dibiayai oleh UMP, hakmiliknya adalah kepunyaan UMP.
2. Naskah salinan di dalam bentuk kertas atau mikro hanya boleh dibuat dengan kebenaran bertulis daripada penulis.
3. Perpustakaan Universiti Malaysia Pahang dibenarkan membuat salinan untuk tujuan pengajian mereka.
4. Kertas projek hanya boleh diterbitkan dengan kebenaran penulis. Bayaran royalti adalah mengikut kadar yang dipersetujui kelak.
5. \*Saya membenarkan/tidak membenarkan Perpustakaan membuat salinan kertas projek ini sebagai bahan pertukaran di antara institusi pengajian tinggi.
6. \*\*Sila tandakan (✓)

SULIT

(Mengandungi maklumat yang berdarjah keselamatan atau kepentingan Malaysia seperti yang termaktub di dalam AKTA RAHSIA RASMI 1972)

TERHAD

(Mengandungi maklumat TERHAD yang telah ditentukan oleh organisasi/badan di mana penyelidikan dijalankan)

TIDAK TERHAD

Disahkan oleh:

\_\_\_\_\_  
(TANDATANGAN PENULIS)

Alamat Tetap: Lot 1140, Bt 5, Jln Sg Tunggul  
Kg Sg Gulang-Gulang,  
45500 Tg Karang, Selangor D. E.

\_\_\_\_\_  
(TANDATANGAN PENYELIA)

**Dr. Mimi Sakinah bt Abd Munaim**  
Nama Penyelia

Tarikh: 3 Disember 2010

Tarikh: 3 Disember 2010

- CATATAN:
- \* Potong yang tidak berkenaan.
  - \*\* Jika tesis ini SULIT atau TERHAD, sila lampirkan surat daripada pihak berkuasa/organisasi berkenaan dengan menyatakan sekali sebab dan tempoh tesis ini perlu dikelaskan sebagai SULIT atau TERHAD.
  - ◆ Tesis dimaksudkan sebagai tesis bagi Ijazah Doktor Falsafah dan Sarjana secara penyelidikan, atau disertai bagi pengajian secara kerja kursus dan penyelidikan, atau Laporan Projek Sarjana Muda (PSM).

“I hereby declare that I have read this thesis and in my opinion this thesis has fulfilled the qualities and requirement for the award of the degree of Bachelor of Chemical Engineering (Biotechnology)”

Signature : .....

Name of supervisor : Dr. Mimi Sakinah bt Abd Munaim

Date : 3<sup>rd</sup> December 2010

**RECOVERY AND SEPARATION OF CELLULOSE FROM SAWDUST WOOD  
HYDROLYSATES USING MEMBRANE REATOR: EFFECT OF  
TRANSMEMBRANE PRESSURE (TMP) AND CROSS FLOW VELOCITY  
(CFV)**

**MOHAMAD AFIS BIN ADNAN**

**A thesis submitted in fulfillment  
of the requirements for the award of the degree of  
Bachelor of Chemical Engineering (Biotechnology)**

**Faculty of Chemical & Natural Resources Engineering  
Universiti Malaysia Pahang**

**DECEMBER 2010**

I declare that this thesis entitled “Recovery and Separation of Cellulose from Sawdust Wood Hydrolysates using Membrane Reactor: Effect of Transmembrane Pressure (TMP) and Cross Flow Velocity (CFV)” is the result of my own research except as cited in references. The thesis has not been accepted for any degree and is not concurrently submitted in candidature of any other degree.”

Signature : .....

Name : Mohamad Afis Bin Adnan

Date : 3<sup>rd</sup> December 2010

*Special dedication of this grateful feelings to my  
beloved father and mother,  
loving brothers and sisters.  
For their loves, supports and best wishes.*

## AKNOWLEDGEMENT

In the name of Allah, the Most Gracious, the Most Merciful.

With the successful completion of my Undergraduate Research Project, first and foremost I would like to give my gratitude to Allah S.W.T because of His blessing, for giving me strength throughout my research.

I would like to take this opportunity to express my sincere thanks and appreciation to my supervisor, Dr. Mimi Sakinah bt Abd Munaim for her guidance, inspiration, patient, encouragement, critics and support in completing my final year project. The publication of this study would not be possible without her advice and encouragement. All lessons, advise and unparalleled knowledge shared would not be forgotten.

I am very thankful to Universiti Malaysia Pahang (UMP) for providing good facilities in the campus. Many thanks to all the technical staff at Faculty of Chemical & Natural Resources Engineering, UMP especially to Mr. Hairul Hisham for his assistance and support during the research in the laboratory.

Exclusive thanks to my family, for their support, encourage and patient throughout my final year project. I am very grateful to have family members that very supportive and understanding especially my mother and my beloved father. Thank you so much. To all my colleagues and friends, thanks for the support and the knowledge that we had shared together.

## ABSTRACT

Cellulose is among the most important natural resources that contain polysaccharides. In this study, the effect of transmembrane pressure (TMP) and cross-flow velocity (CFV) on permeate flux during the recovery and separation of cellulose from sawdust wood hydrolysates by using membrane reactor was investigated. Two-stage pretreatment was performed by using dilute sodium hydroxide (NaOH) and followed by dilute sulfuric acid (H<sub>2</sub>SO<sub>4</sub>) for about 24 hours at 75°C respectively. Separation of cellulose from sawdust wood hydrolyzed was performed by using ceramic microfiltration membrane with pore size of 0.9µm and effective surface area of approximately 0.03m<sup>2</sup> for 60 minutes at 50°C respectively. The experiment was conducted at five different values of TMP and CFV range from 0.5 to 2.5 bars and 0.02 to 0.18 m/s. During the filtration experiments, the permeate flux through microfiltration membrane was relatively high. At first, the highest flux was found at an optimum TMP and CFV of 1.5 bars and 0.14 m/s with percentage of flux decline at 2.68% and 11.75% respectively. After optimization using Response Surface Methodology (RSM), the maximum permeate flux obtained was at 247.614 L/m<sup>2</sup>.h at an optimum TMP of 1.0 bar and optimum CFV of 0.14 m/s within the duration of 20 minutes of filtration. As conclusion, TMP and CFV give significant effect on permeate flux.

## ABSTRAK

Sellulosa merupakan antara sumber asli yang terpenting yang mengandungi polisakarida. Dalam kajian ini, kesan tekanan transmembran (TMP) dan halaju berlawanan arus (CFV) terhadap fluk semasa pemulihan dan pengasingan sellulosa daripada hasil hidrolasi habuk kayu dengan menggunakan reaktor membran telah dikaji. Dua peringkat pra-rawatan telah dilakukan dengan menggunakan sodium hidroksida cair (NaOH) dan diikuti dengan pra-rawatan menggunakan asid sulfurik cair ( $H_2SO_4$ ) selama 24 jam pada suhu  $75^\circ C$  setiap satu. Pengasingan sellulosa daripada hasil hidrolasi habuk kayu dilakukan dengan menggunakan membran penapis mikro jenis seramik dengan saiz liang  $0.9 \mu m$  yang mempunyai keluasan permukaan efektif menghampiri  $0.03 m^2$  selama 60 minit pada suhu  $50^\circ C$  setiap satu. Eksperimen telah dijalankan pada lima nilai TMP dan CFV yang berbeza dalam lingkungan 0.5 hingga 2.5 bar dan 0.02 hingga 0.18 m/s. Semasa eksperimen penapisan, fluk yang melalui membran penapis mikro adalah tinggi secara relatif. Pada awalnya, fluk tertinggi telah dikenalpasti pada nilai optimum TMP dan CFV pada 1.5 bar dan 0.14 m/s dengan peratus kejatuhan fluk sebanyak 2.68% dan 11.75% setiap satu. Selepas pengoptimuman menggunakan kaedah tindakbalas permukaan (RSM), fluk maksimum terhasil adalah sebanyak  $247.614 L/m^2.h$  pada nilai optimum TMP dan CFV pada 1.0 bar dan 0.14 m/s setiap satu dalam jangkamasa 20 minit penapisan. Kesimpulannya, TMP dan CFV memberi kesan signifikan terhadap fluk.

## TABLE OF CONTENTS

<b>CHAPTER</b>	<b>TITLE</b>	<b>PAGE</b>
	<b>TITLE</b>	i
	<b>DECLARATION</b>	ii
	<b>DEDICATION</b>	iii
	<b>ACKNOWLEDGEMENT</b>	iv
	<b>ABSTRACT</b>	v
	<b>ABSTRAK</b>	vi
	<b>TABLE OF CONTENTS</b>	vii
	<b>LIST OF TABLES</b>	x
	<b>LIST OF FIGURES</b>	xi
	<b>LIST OF SYMBOLS, NOMENCLATURE AND ABBREVIATIONS</b>	xiii
	<b>LIST OF APPENDICES</b>	xiv
<b>1</b>	<b>INTRODUCTION</b>	<b>1</b>
	1.1 Background of Study	1
	1.2 Problem Statement	2
	1.3 Research Objectives	3
	1.4 Scope of the Study	3
	1.5 Significance of the Study	4
<b>2</b>	<b>LITERATURE REVIEW</b>	<b>5</b>
	2.1 Sources of Lignocellulosic Biomass	5

2.2	Pretreatment and Recovery of Lignocellulosic Biomass	8
2.3	Cellulose (Product)	13
2.4	Separation of Lignocellulosic Biomass Recovery	14
2.5	Membrane Process	15
2.6	Membrane Separation of Cellulose	15
2.6.1	Microfiltration	19
2.6.2	Ultrafiltration	19
2.6.3	Nanofiltration	21
2.6.4	Reverse Osmosis	22
2.7	Membrane Fouling	23
2.7.1	Effect of Cross Flow Velocity (CFV)	24
2.7.2	Effect of Transmembrane Pressure (TMP)	25
2.8	Membrane Cleaning	25
2.9	Response Surface Methodology (RSM)	27
<b>3</b>	<b>METHODOLOGY</b>	<b>28</b>
3.1	General Methodology	28
3.2	Preparation of Raw Material	29
3.3	Two stage of Pretreatment Process	31
3.3.1	Sodium Hydroxide (NaOH) pretreatment	31
3.3.2	Sulfuric Acid (H <sub>2</sub> SO <sub>4</sub> ) pretreatment	33
3.4	Membrane Separation of Cellulose	34
3.5	Membrane Cleaning	36
3.6	Optimization of Separation of Cellulose Recovery using Response Surface Methodology	38
<b>4</b>	<b>RESULT AND DISCUSSION</b>	<b>39</b>
4.1	Introduction	39
4.2	Effect of Transmembrane Pressure (TMP) on Flux	39
4.3	Effect of Cross Flow Velocity (CFV) on Flux	46
4.4	Optimization of Separation of Cellulose Recovery	52

	using Response Surface Methodology	
4.4.1	ANOVA Analysis	54
4.4.2	Effect of Interactions of TMP-CFV and CFV-Time on Flux	57
<b>5</b>	<b>CONCLUSION AND RECOMMENDATION</b>	<b>63</b>
5.1	Conclusion	63
5.2	Recommendation	64
	<b>REFERENCES</b>	<b>65</b>
	<b>APPENDIX A</b>	<b>71</b>
	<b>APPENDIX B</b>	<b>73</b>

**LIST OF TABLES**

<b>TABLE NO.</b>	<b>TITLE</b>	<b>PAGE</b>
2.1	Cellulose, Hemicelluloses and Lignin contents in lignocellulosic biomass	6
2.2	Pretreatment methods for lignocellulosic biomass	10
3.1	Low and high values for optimization in Response Surface Methodology	38
4.1	Design layout and experimental results	53
4.2	Regression coefficient and <i>P</i> -value calculated from the model	55
4.3	ANOVA for response surface model	56
4.4	ANOVA table (partial sum of square) for quadratic model (response flux)	56

**LIST OF FIGURES**

<b>FIGURE NO.</b>	<b>TITLE</b>	<b>PAGE</b>
2.1	Sources of lignocellulosic biomass	5
2.2	Sawdust from sawmill	7
2.3	Schematic of the role of pretreatment in conversion of biomass	9
2.4	Structure of cellulose	13
2.5	Ranges for separation process	17
2.6	Separation characteristics for pressure driven membranes	18
3.1	Process flow for recovery and separation of cellulose	28
3.2	Sawdust taken from sawmill factory	29
3.3	Sawdust after grinder and sieved	30
3.4	Sawdust after drying	30
3.5	Sodium hydroxide (NaOH) pretreatment in membrane reactor	32
3.6	Sawdust (solid residue) after pretreatment process	32
3.7	Pretreated sawdust (NaOH pretreatment) being introduced into membrane reactor	33
3.8	Sulfuric acid (H <sub>2</sub> SO <sub>4</sub> ) pretreatment in membrane reactor	34
3.9	Membrane reactor system	35
3.10	Parameter adjustment and product collection	36

3.11a	Membrane appearance and sample before filtration process	37
3.11b	Membrane appearance and sample after filtration process	37
3.12	Backwashing using water	37
3.13	Chemical cleaning using 0.05M NaOH	38
4.1	Flux pattern at TMP of 0.5 bar	40
4.2	Flux pattern at TMP of 1.0 bar	41
4.3	Flux pattern at TMP of 1.5 bars	42
4.4	Flux pattern at TMP of 2.0 bars	43
4.5	Flux pattern at TMP of 2.5 bars	44
4.6	Comparison of permeate flux at different TMP	45
4.7	Flux pattern at CFV of 0.02 m/s	46
4.8	Flux pattern at CFV of 0.06 m/s	47
4.9	Flux pattern at CFV of 0.10 m/s	48
4.10	Flux pattern at CFV of 0.14 m/s	49
4.11	Flux pattern at CFV of 0.18 m/s	50
4.12	Comparison of permeate flux at different CFV	51
4.13	Normal probability plot of residual for flux	57
4.14	Plot of residual vs. predicted response for flux	58
4.15	Plot of outlier T vs. run for flux	59
4.16	3-D surface plot on flux for interaction of TMP (A) and CFV (B)	60
4.17	3-D surface on flux rate for interaction of CFV (B) and Time (C)	61

**LIST OF SYMBOL, NOMENCLATURE AND ABBREVIATION**

$\alpha$	Alpha
$\beta$	Beta
$^{\circ}\text{C}$	Celcius
A	Effective membrane area, $\text{m}^2$
ANOVA	Analysis of variance
CCD	Central composite design
CFV	Cross flow velocity
$\text{H}_2\text{SO}_4$	Sulfuric acid
HCl	Hydrochloric acid
J	Flux
kDa	kilo Dalton
$\text{L}/\text{m}^2.\text{h}$	Liter per meter square per hour
M	Molarity
MWCO	Molecular Weight Cut-Off
NaOH	Sodium hydroxide
Q	Permeate flow rate in liter per minute
rpm	Revolution per minute
RSM	Response Surface Methodology
R	Correlation coefficient
$R^2$	Determination coefficient
TMP	Transmembrane pressure

**LIST OF APENDICES**

<b>APPENDIX</b>	<b>TITLE</b>	<b>PAGE</b>
A	Preparation of Alkali and Acid solutions	71
B	Calculation of permeate flux during separation process	73

## CHAPTER 1

### INTRODUCTION

#### 1.1 Background of Study

Lignocelluloses biomass primarily consists of cellulose, hemicelluloses, and lignin which are usually being used as raw materials in the production of ethanol. Lignocelluloses biomass is believed to be less expensive and more plentiful than either starch or sucrose containing feedstock. Forest residues such as sawdust and wood bark are believed to be one of the most abundant sources of sugars, although much research has been reported on herbaceous grass such as switch grass, agricultural residue such as corn stover and municipal waste (Hu *et al.*, 2008).

Besides that, the polysaccharides namely; cellulose and hemicelluloses present in the lignocelluloses biomass need to be hydrolyzed with acids or enzymes in order to produce fermentable sugars. Pretreatment is an important tool for practical cellulose conversion processes. Pretreatment is required to alter the structure of cellulosic biomass to make cellulose more accessible to the enzymes that convert the carbohydrate polymers into fermentable sugars. Several studies have shown the potential of sodium hydroxide pretreatment on a variety of lignocellulosic materials. Sodium hydroxide pretreatment can enhance lignocelluloses digestibility by increasing internal surface area, decreasing the degree of polymerization and the crystallinity of celluloses, and

separating structural linkages between lignin and carbohydrates effectively which will decreased lignin content (Wang *et al.*, 2010). Apart from that, dilute acid pretreatment has been widely investigated due to its effectiveness and inexpensive method of pretreatment compared to other pretreatment methods. The dilute sulfuric acid pretreatment can effectively solubilized hemicelluloses into monomeric sugars and soluble oligomers, thus improving cellulose conversion (Sun and Cheng, 2005). Thus, the combination of this two pretreatment to recovery of celluloses from different biomasses especially from wood will be one of the most interesting industrial processes in the near future.

In biotechnology industries, membrane application is gradually emerge as a powerful bioseparation for purification, fractionation, separation and concentration of bioproducts (Sakinah *et al.*, 2008). Pressure driven membrane filtration, one of membrane separation processes has been used to separate and concentrate the hemicelluloses extracted from wood (Mohammad, 2008). This procedure could be used for the cellulose separation. Membrane processes are generally classified into different categories which ranging from reverse osmosis and nanofiltration to ultrafiltration and cross-flow microfiltration that could be used to separate the cellulose.

The combination of membrane separation and reactor is known as membrane reactor (MR), which found to be capable to separate products from reaction mixture by using the membrane filter as well as to retain the ash and reject the solute with larger molecular weight (MW) than the molecular weight cut-off (MWCO) of the membrane (Sakinah *et al.*, 2007).

## **1.2 Problem Statement**

Membrane filtration was one of the applications in separation process but normally in membrane filtration process, membrane fouling is the most difficult and

complicated problem to be manage. Membrane fouling occurs due to solute adsorption, particle interception or membrane blocking (Hwang and Sz, 2010).

Membrane fouling can cause many problems in industries such as operational problem of membrane installations (e.g. increase of pressure drop and/or decrease of flux) and increase the plant operational cost. Factors which lead to membrane fouling are membrane material properties, the feed characteristic and the operating parameters.

### **1.3 Research Objectives**

The objectives of this research are to study the effect of transmembrane pressure (TMP) and cross-flow velocity (CFV) on permeate flux during the recovery and separation of cellulose from sawdust wood hydrolysates using membrane reactor, to determine an optimum TMP and CFV during membrane filtration and also to optimize the effect of TMP and CFV on flux using Response Surface Methodology (RSM).

### **1.4 Scope of Study**

In order to achieve the objective of the research, the optimum operating parameters; and flux during separation process will be observed. The optimum operating condition (transmembrane pressure (TMP), cross flow velocity (CFV)) is important to obtain the high flux of cellulose recovery with less possibility of membrane fouling. The separation process is performed at the operating condition of TMP and CFV at a range from 0.5 to 2.5 bars and 0.02 to 0.18 m/s respectively.

## 1.5 Significance of the Study

Raw material used can be considered as a low cost because sawdust was abundant and inexpensive in Malaysia. The composition of the cellulose is plenty in sawdust. The reuse of sawdust can also reduce the environmental pollution. Besides that, the production of cellulose has a potential in a future because from the cellulose, many valuable product can be produce such as bio-ethanol.

In addition, recovery and separation of cellulose from sawdust hydrolysates by membrane separation using membrane reactor has not been studied. This will give an economical advantage since it is simple process with low energy requirement (Faria *et al.*, 2002). Otherwise, the effect of transmembrane pressure (TMP) and cross flow velocity (CFV) during the separation process can prevent slow permeate flow rate due to the occurrence of membrane fouling. Hence, by controlling and adjusting the TMP and CFV the optimum permeate flux can be obtained.

## CHAPTER 2

### LITERATURE REVIEW

#### 2.1 Sources of Lignocellulosic Biomass

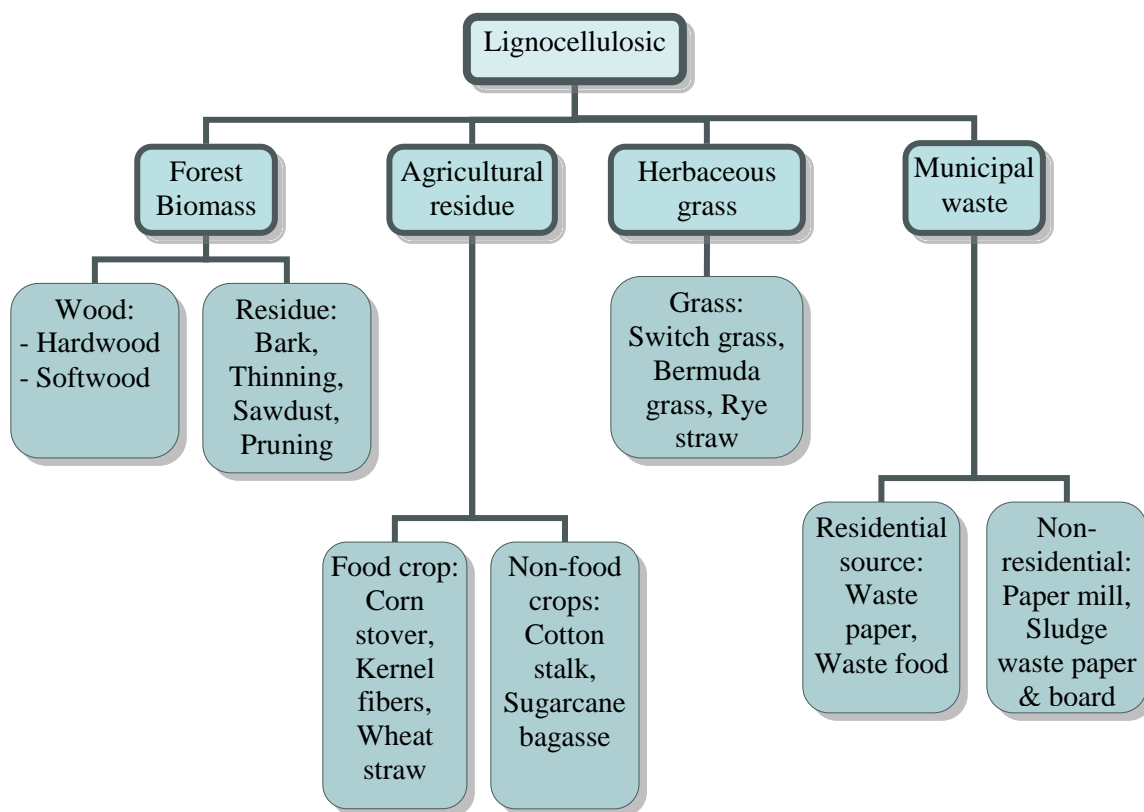


**Figure 2.1:** Sources of lignocellulosic biomass.

Figure 2.1 shows several sources of lignocellulosic biomass. In general, prospective lignocellulosic materials for fuel ethanol production can be divided into six main groups namely crop residues such as sugarcane bagasse, corn stover, wheat straw, rice straw, rice husks, barley straw, sweet sorghum bagasse, olive stones and pulp, hardwood such as aspen and poplar, softwood such as pine and spruce, cellulose wastes such as newsprint, waste office paper and recycled paper sludge, herbaceous biomass such as alfalfa hay, switch grass, reed canary grass, coastal Bermudagrass and timothy grass.

Lignocellulosic biomass typically contains 55–75% carbohydrates by dry weight (Mosier *et al.*, 2005). The carbohydrate content consists of mainly three different types of polymers, namely cellulose, hemicelluloses and lignin, which are associated with each other (Hendriks and Zeeman, 2009). Table 2.1 shows the general composition of selective lignocellulosic biomass containing cellulose, hemicelluloses and lignin.

**Table 2.1:** Cellulose, Hemicelluloses and Lignin contents in lignocellulosic biomass  
(Kumar *et al.*, 2009)

Lignocellulosic material	Cellulose (%)	Hemicelluloses (%)	Lignin (%)
Hardwood stems	40-55	24-40	18-25
Softwood stems	45-50	25-35	25-35
Nut shells	25-30	25-30	30-40
Corn cobs	45	35	15
Grasses	25-40	35-50	10-30
Paper	85-99	0	0-15
Wheat straw	30	50	15
Sorted refuse	60	20	20
Leaves	15-20	80-85	0
Cotton seed hairs	80-95	5-20	0
Newspaper	40-55	25-40	18-30
Waste papers from chemical pulps	60-70	10-20	5-10
Primary wastewater solids	8-15		
Solid cattle manure	1.6-4.7	1.4-3.3	2.7-5.7
Coastal Bermudagrass	25	35.7	6.4
Switch grass	45	31.4	12
Swine waste	6	28	N/A

Nowadays, a large quantity of cellulosic waste products was discarded from the forest product industry because it cannot be utilized as food in its present forms. Woody biomass for example is sustainability available in large quantities in various region of the world. Besides that, woody biomass such as sawdust (Figure 2.2) was containing 70% to 80% carbohydrates. Furthermore, woody biomass has higher lignin content and also physically larger and structurally stronger and denser (Zhu and Pan, 2010).



**Figure 2.2:** Sawdust from sawmill.

Sawdust is a waste by-product of the timber industry that is either used as a packing material. It is believed to be composed of those three important constituents such as cellulose, lignin, and hemicelluloses. Sawdust is not only abundant, but also has advantage to be used an efficient adsorbent that is effective to many types of pollutants, such as dyes, oil, salt and heavy metals (Batzias and Sidiras, 2007).

## 2.2 Pretreatment and Recovery of Lignocellulosic Biomass

Lignocellulosic biomass is mainly composed of cellulose, hemicelluloses and lignin. Cellulose was hydrolyzed to its monomeric constituents during enzymatic hydrolysis and then fermented to ethanol or other products. The cellulose biodegradation by cellulolytic enzymes is slow because of the networks between lignin-hemicelluloses were embedded the cellulose fibers. Therefore, pretreatment process is important to remove lignin and hemicelluloses, reduce cellulose crystallinity, and increase the porosity of the materials (Sun and Cheng, 2002) so that the produced cellulose is suitable for enzymatic hydrolysis.

Pretreatment is required to disrupt the structure of lignocellulosic materials during cellulosic ethanol production, because the extensive interactions among cellulose, hemicelluloses and lignin, and the barrier nature of lignin minimize enzyme access to the carbohydrates and result in poor yields of fermentable sugars. Figure 2.3 show the schematic of the role of pretreatment in conversion of biomass.

In general, pretreatment methods can be roughly divided into different categories such as physical pretreatment (e.g.: milling and grinding), physicochemical pretreatment (e.g. steam pretreatment/autohydrolysis, hydrothermalolysis, and wet oxidation), chemical pretreatment (e.g. alkali, dilute acid, oxidizing agents, and organic solvents), biological, electrical, or a combination of these. The following pretreatment technologies have promise for cost-effective pretreatment of lignocellulosic biomass for biological conversion to fuels and chemicals (Kumar *et al.*, 2009). Some pretreatment combines any two or all of these pretreatment and can be produce subcategories.

Biological pretreatment has not attach much attention probably because of kinetic and economic considerations although there have been various research showing biological pretreatment can be an effective way to recover sugars from different species of biomass.

Physical and chemical pretreatments have been the subject of intensive research. Steam and water are usually excluded from being considered as chemical agent for pretreatment, since no extra chemical are added to the biomass. Physical pretreatment include comminuting, in which the particle sizes of the biomass are reduced with mechanical forces, steam explosion, and hydrothermalolysis.

Acids or bases promote hydrolysis and improve sugar recovery yield from cellulose by removing hemicelluloses and lignin during pretreatment. Sulfuric acid and sodium hydroxide are the most commonly used acid and base, respectively. Another approach for pretreatment is to use liquid formulations capable for acting as solvent for cellulose. Works with cellulose solvent systems have shown the enzymatic hydrolysis could be greatly improved, but the works mainly have been restricted to agricultural residues and herbaceous grass. Other methods for pretreatment of lignocelluloses biomass is shown in Table 2.2.

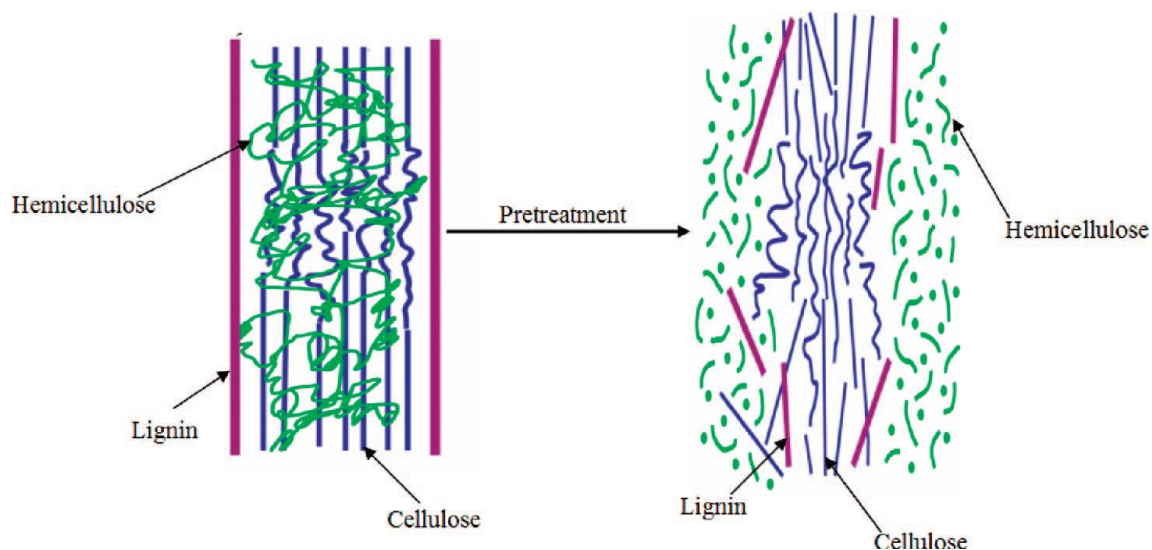


**Figure 2.3:** Schematic of the role of pretreatment in conversion of biomass (Kumar *et al.*, 2009).

**Table 2.2:** Pretreatment methods for lignocellulosic biomass

Pretreatment	Energy		Effect
	Source	Means	
Biological pretreatment	Microbe	Fungi	Reduce DP of cellulose and hemicelluloses
		Actinomycetes	Remove lignin
Physical pretreatment	Comminution	Ball Milling	Decrease particle size, cellulose crystallinity & DP
		Colloid Milling	
		Hammer Milling	
		Compression Milling	
	Irradiation	Electron Beam	Increase surface area and pore size Soften partially depolymerize lignin
		Gamma-ray	
		Microwave	
	Hydrothermolysis	Liquid Hot Water	Partially hydrolyze hemicellulose
	Steam explosion	High Pressure Steam	
Other mechanical energy	Expansion		
	Extrusion		
Chemical pretreatment	Acid	Carbonic acid	Decrease crystallinity of cellulose and its DP Partial or complete hydrolyze hemicelluloses Delignification
		Hydrochloric acid	
		Hydrofluoric acid	
		Nitric acid	
		Peracetic acid	
		Phosphoric acid	
		Sulfur dioxide	
		Sulfuric acid	
	Alkaline	Lime	
		Sodium hydroxide	
		Sodium carbonate	
		Ammonia	
		Ammonium sulfite	
	Gas	Chlorine dioxide	
		Nitrogen dioxide	
	Oxidant	Hydrogen peroxide	
		Ozone	
		Wet oxidation	
	Cellulose solvent	Cadoxen	
		CMCS	
DMSO			
Extraction of lignin	Hydrozine		
	Ethanol-Water		
	Benene-Water		
	Ethylene glycol		
	Butanol-Water		
	Swelling agent		

One of the main problems during the pretreatment and hydrolysis of biomass is the variability in the content of lignin and hemicelluloses. This variability depends on factors as the type of plant from which the biomasses obtained, crop age, method of harvesting, etc. this makes that no one of the pretreatment methods could be applied in a generic way for many different feed stocks. The future trends for improving the pretreatment of lignocellulosic feed stocks also include the production of genetically modified plant materials with higher carbohydrate content or modified plant structure to facilitate pretreatment in milder conditions or using hemicellulases.

Several studies have shown the potential of sodium hydroxide pretreatment on a variety of lignocellulosic materials. Furthermore, sodium hydroxide can enhance lignocelluloses digestibility by increasing internal surface area, decreasing the degree of polymerization and the crystallinity of celluloses, and separating structural linkages between lignin and carbohydrates effectively. Besides that, the digestibility of sodium hydroxide treated hardwood increased with the decrease of lignin content (Wang *et al.*, 2010).

Otherwise, the porosity of the lignocellulosic materials increases with the removal of the cross links which is lignin (Sun and Cheng, 2002). The major effect of alkaline pretreatments is the delignification of lignocellulosic biomass, thus enhancing the reactivity of the remaining carbohydrates (Wang *et al.*, 2010).

Besides that, based on the prominently researched and promising technology, dilute acid pretreatment was chosen as the method for treatment. The function of acid in this pretreatment is to break down the hemicelluloses and opens the remaining structure for subsequent enzymatic hydrolysis. Furthermore, reaction conditions which favor the production of xylose monomer while minimizing degradation to furfural is preferred so as they do not inhibit subsequent enzymatic hydrolysis.

Pretreatment of biomass with dilute sulfuric acid at high temperatures can effectively dissolve the hemicelluloses and increase the enzymatic digestibility of celluloses. Beside that, the pretreatment can be performed at the moderate temperature. These two conditions give different xylose yield as well as the glucose yield. However, the dilute acid pretreatment still give significant results based on the production of xylose and glucose. The reaction time can be extended to obtained higher yield of sugar with a period from days to week. The advantages of the dilute sulfuric acid were high reaction rates, low acid consumption, and low cost of sulfuric acid. Dilute sulfuric acid pretreatment is deserving attention due to relatively inexpensive and to produce high hemicelluloses recoveries and cellulose digestibilities (Lee *et al.*, 2009). Therefore it has been assayed on a variety of substrates.

The application of dilute acid pretreatment to woody biomass can achieve some level of success so that can provide satisfactory cellulose conversion with certain hardwood species (Zhu and Pan, 2009). The dilute sulfuric acid pretreatment can effectively solubilized hemicelluloses into monomeric sugars, thus improving cellulose conversion. Compared to other pretreatment methods, it is especially useful for the conversion of xylan in hemicelluloses to xylose that can be further fermented to ethanol by many microorganisms (Sun and Cheng, 2005).

Otherwise, dilute sulfuric acid pretreatment is effective because it is relatively inexpensive and due to high hemicelluloses recovery and cellulose digestibility's (Cara *et al.*, 2008). Besides that, dilute acid pretreatment with sulfuric acid has been extensively researched because it is inexpensive and effective, although other acid such as nitric acid, hydrochloric acid and phosphoric acid has also been tested (Hu *et al.*, 2008).

### 2.3 Cellulose (Product)

Cellulose is the main structural constituent in plant cell walls and is found in an organized fibrous structure. In herbaceous and woody plants, cellulose exists as linear polymer of glucose. Besides that, cellulose also associated with another polysaccharide, hemicelluloses and seal with lignin which is a complex three dimensional polychromatic compound that is resistant to enzyme and acid hydrolysis.

Cellulose exists of D-glucose subunits, linked by  $\beta$ -1,4 glycosidic bonds (Figure 2.4). In plants, there are consists of two parts of cellulose, which organized part and unorganized part. The organized part contained a crystalline structure and another part contained amorphous structure. Cellulose fibrils or cellulose bundles were the cellulose strains that ‘bundled’ together. These cellulose fibrils are mostly independent and weakly bound through hydrogen bonding (Hendriks and Zeeman, 2008).

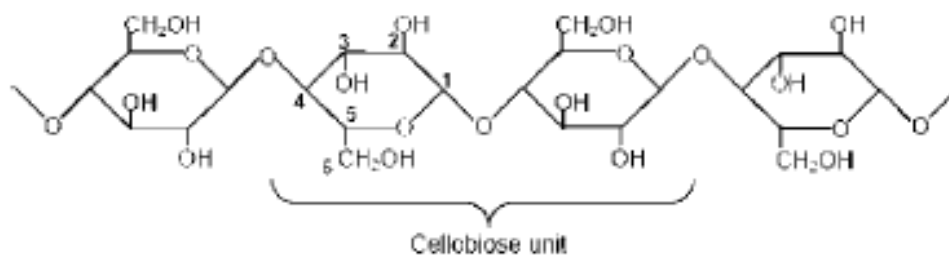


**Figure 2.4:** Structure of cellulose (Kumar *et al.*, 2009).

Cellulose, like starch, is a polymer of glucose. However, unlike starch, the specific structure of cellulose favors the ordering of the polymer chains into tightly packed, a highly crystalline structure that is water insoluble and resistant to depolymerization (Mosier *et al.*, 2005).

## 2.4 Separation of Lignocellulosic Biomass Recovery

The biorefinery has been projected as a facility for the sustained processing of biomass into a spectrum of commercially viable products. Forest biorefineries are expected to process forest biomass feedstock such as wood into a spectrum of fuel and material products, similar to the operation of conventional petroleum refineries. In the forest biorefinery, wood is hydrolyzed to extract some of the hemicelluloses after which it is sent further to the conventional pulping and bleaching process to make papermaking pulps (Duarte *et al.*, 2010).

Separation processes such as sedimentation, filtration, membrane separation and centrifugal separations can be used for fractionating the wood extract. For the success of any molecular or ionic separation process downstream from wood hydrolysis and extraction, the extracts must be relatively clean and particles free (Duarte *et al.*, 2010). This is particularly important since fouling and flux decay in nanofiltration or reverse osmosis applications can render these separations unviable on large scale.

Research has been conducted by Alriols *et al.*, (2010) on the combined organosolv ethanol pretreatment with membrane ultrafiltration technology to treat the non-woody biomass feedstock of the species *miscanthus sinensis*. The lignin fraction with specific molecular weight was obtained by membrane ultrafiltration as it proportioned excellent fractionation capability with low chemicals consumption and low energy requirements.

Besides that, acetic acid produced from the hydrolysis of herbaceous biomass such as corn stover was conventionally being separate and removed by chromatography method using resin column. Due to certain limitation, adsorptive microporous membrane has been used to remove acetic acid from corn stover hydrolysates (Wickramasinghe *et al.*, 2008).

Furthermore, the separation of hemicelluloses from wood hydrolysates has been reported (Mohammad, 2008). The retention of hemicelluloses using two filtration steps was found to almost complete where the fouling ability of the used membrane was relatively low. The flux obtained at the first filtration was  $165 \text{ kg/m}^2\cdot\text{h}$  at 1 bar with 18% of membrane fouling and  $24 \text{ kg/m}^2\cdot\text{h}$  of flux at 10 bars with 30% of membrane fouling at second filtration.

## **2.5 Membrane Process**

Membrane processes are mass transfer unit operations utilized for separation process either liquid-liquid or gas-liquid mixtures. Membrane is an ultra thin semi permeable barrier separating two fluids and allows the transport of certain species through the barrier from one fluid to the other. It is this permeability that gives the membrane its utility and potential to separate a variety of process streams. The most universally employed membranes are composed of organic polymers.

Otherwise, type of membrane from metal, ceramic, liquid and gas membranes are also used. In all membrane methods, the membrane separates the fluid passing through it into a permeate (that which passes through) and a retentate (that which is left behind). When the membrane is chosen so that it is more permeable to one constituent than the other, then permeate will be richer in the first constituent than the retentate (Kumar *et al.*, 2010).

## **2.6 Membrane Separation of Cellulose**

Color removal from sugar syrup and the improvement of its sugar purity using ultrafiltration has great advantage. Membrane separation has been studied for color removal from green sugar syrup (Gyura *et al.*, 2005). Ultrafiltration membranes with porosity ranging from 6 to 20 kilo Dalton (kDa) were used to remove color from raw

sugar cane solution. The permeate was decolorized by 58% using a 6 to 8 kDa membrane at a flux of 35.32 L/m<sup>2</sup>.h, which gave the best results. The 15 to 20 kDa membrane only removed 50% of the color at a flux of 15.78 L/m<sup>2</sup>.h.

Membrane separation has been performed as an alternative method for the recovery of xylitol from the fermentation broth of hemicelluloses hydrolysates because it has the potential for energy savings and higher purity (Affleck, 2000). A 10,000 nominal molecular weight cutoff (MWCO) polysulfone membrane was found to be the most effective for the separation and recovery of xylitol. The membrane allowed 82.2 to 90.3% of xylitol in the fermentation broth to pass through the membrane.

Otherwise, membrane filtration has also been used as an alternative for the separation and purification of hemicelluloses extracted from wood and annual crops (Mohammad, 2008). The outcome shows that the permeate flux through ultrafiltration and tight ultrafiltration membranes was relatively high. The fouling ability of the used membranes was relatively low. In addition, the retention of hemicelluloses using two filtration steps was almost complete.

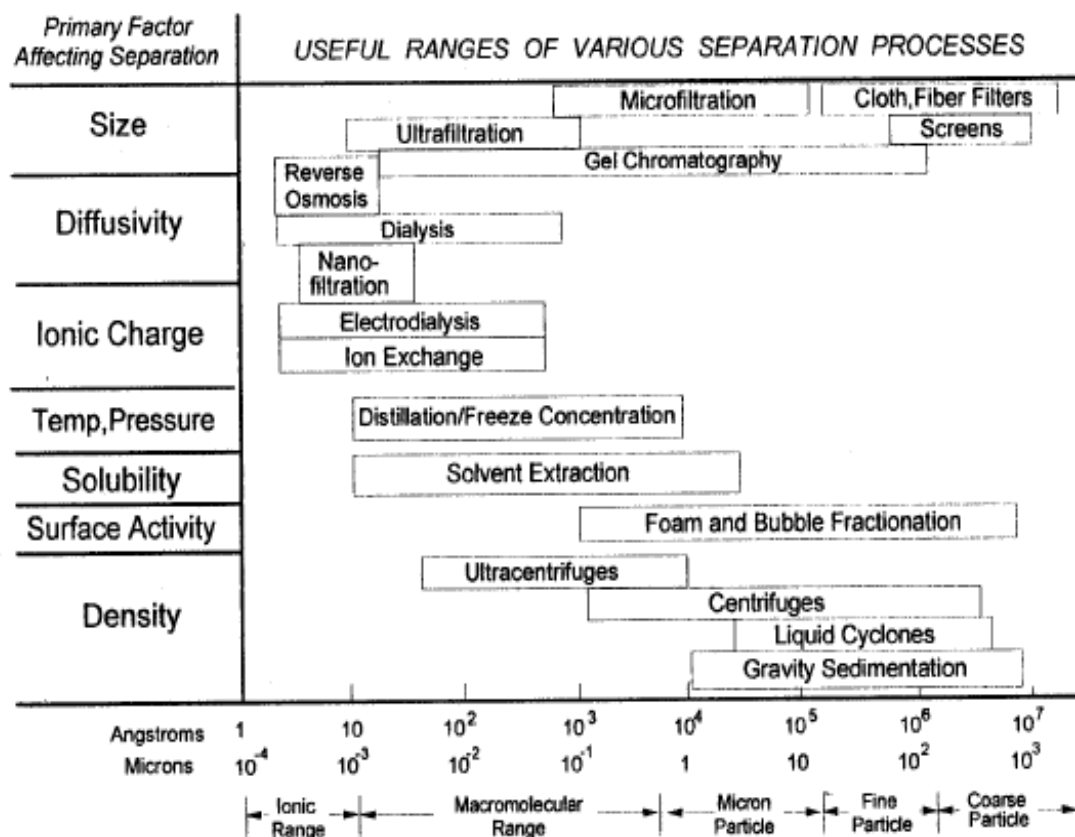


**Figure 2.5:** Ranges for separation process (Affleck, 2000).

Membrane technology is used to recycle the valuable materials and purify the process water for reuse purposes in pulp and paper industry. Several related studies performed membrane filtration to isolate hemicelluloses from process water of thermo-mechanical pulping.

The membranes available were different in types and come in variety of characteristics which depend on membrane material and the process condition during manufacture. The nominal molecular weight cutoff and pore size defines some membranes performances. Membranes will reject certain molecules based on its categorized. Each membrane category can be used to filter solutions and perform different separation tasks. Membranes are generally classified into the categories ranging from microfiltration and ultrafiltration to nanofiltration and reverse osmosis (Figure 2.5).

The major differences between each of these categorized membranes are the nominal molecular weight cutoff (MWCO). The MWCO is based on the spherical shape of the protein molecules and can change with different shape molecules such as, polysaccharides (Affleck, 2000). Microfiltration membranes are classified with pore size ranging from 0.1  $\mu\text{m}$  to 5  $\mu\text{m}$ . Ultrafiltration membranes are classified with pore sizes up to 100 nm which used to reject molecules with molecular weight above 1000. Nanofiltration membranes have MWCO ranging from 300 to 1000, while reverse osmosis membranes are used for removing salts and larger impurities. Figure 2.6 shows the separation characteristics for pressure driven membranes.

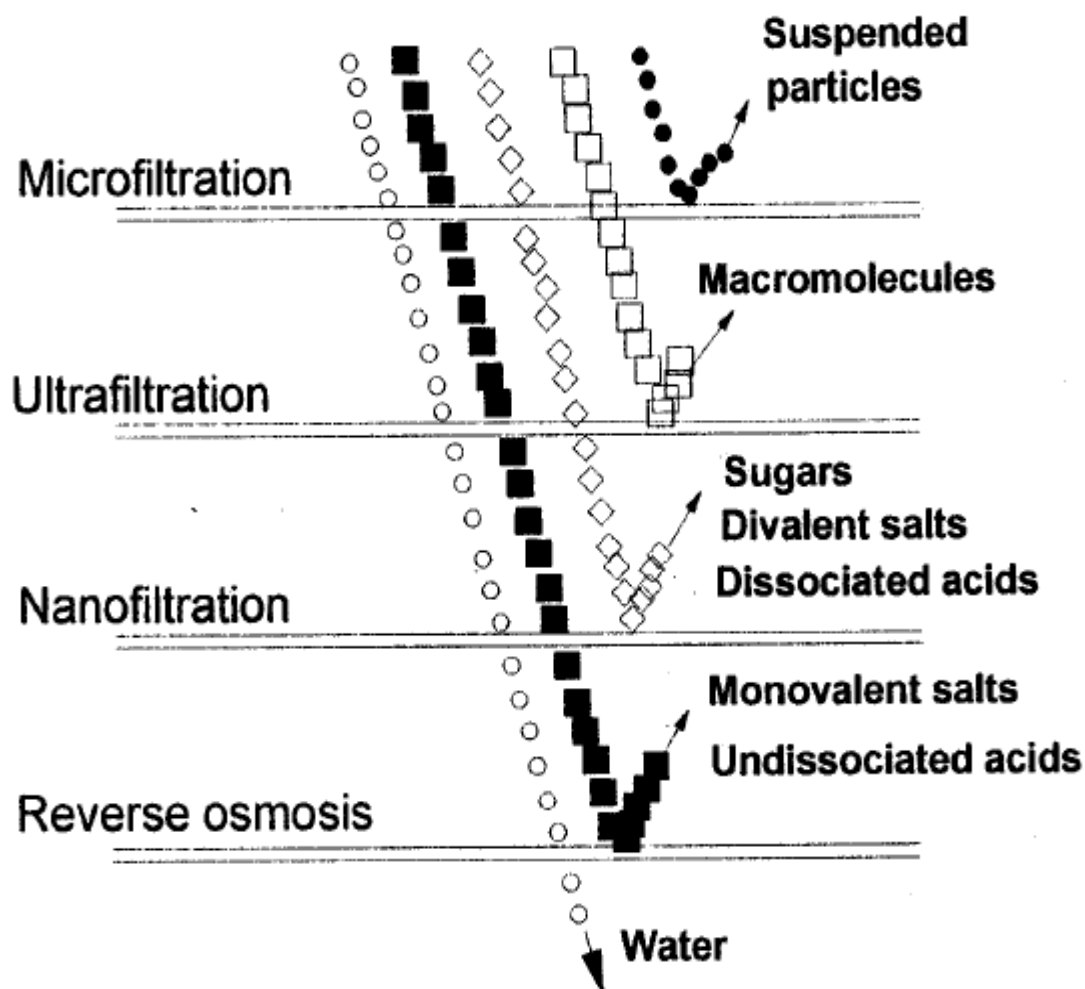


**Figure 2.6:** Separation characteristics for pressure driven membranes (Affleck, 2000).

### **2.6.1 Microfiltration**

This membrane process closely resembles conventional filtration. Microfiltration (MF) can be used to separate suspended particles from solutions. The membranes are designed to reject particles in the micron range from 0.1  $\mu\text{m}$  to 5  $\mu\text{m}$  that means the suspensions and emulsions can be retained. The separation is usually based on solute particles dimensions specifically size and shape. MF can be used for removing particles from liquid or gas streams, purification of water, clarification and wastewater treatment (Affleck, 2000). Removal of suspended solids is the typical application of microfiltration. It can be used as cleaning step in clarification of fruit juice or cold sterilization of beverages and pharmaceutical and also as concentration step such as cell harvesting (Mohammad, 2008). Microfiltration is sometimes used as a pre-treatment step for nanofiltration and reverse osmosis for the production of potable water from ground or surface water, and ultra-pure water in the semiconductor industry.

Materials used to make microfiltration membranes include polypropylene, regenerated cellulose and polyvinyl chloride. Synthetic polymeric membranes can be divided into two classes which are hydrophobic and hydrophilic. The fouling tendency is higher in hydrophobic membrane, especially in proteins separation. Furthermore, water can not pass through some very hydrophobic membranes so they can not be wetted by water. In this case, alcohol can be good alternative to pretreat this membranes prior use them with aqueous solutions (Mohammad, 2008).

### **2.6.2 Ultrafiltration**

Ultrafiltration can be broadly defined as a method for concentrating and fractionating macromolecules where a membrane acts as a selective barrier. Ultrafiltration employs membranes whose pore size typically ranges from 5 to 100 nm, with a MWCO above 1,000. Polysulfone and polyethersulfone are commonly used to make ultrafiltration membranes. Some factors that affect the separation in ultrafiltration

membranes are the membrane type and characteristics, transmembrane pressure, pH of the feed, and the protein concentration in the feed (Affleck, 2000).

Materials and conditions used can control how large the pores of the membrane are and consequently what molecules and particles can pass through the membrane. The transmembrane pressure is the driving force for flux and is measured as the average of the inlet and outlet pressure, minus the pressure on the permeate side of the membrane. Permeate rates are measured in flux, which is the amount of fluid passing through the membrane and is usually given in terms of volume per unit time per unit membrane area (Affleck, 2000). From Equation 1, the parameters applied to identify the flux declination and the efficiency of membrane processes are as follows:

$$J = \frac{Q}{A} \quad (\text{Equation 2.1})$$

where  $J$  is the flux through the membrane (LMH),  $Q$  is the permeate flow rate (LPM) and  $A$  is the effective membrane area ( $\text{m}^2$ ) (Sakinah *et al.*, 2007).

The membrane separation of cheese whey was evaluated by using two criteria which are permeate flux and protein retention. From Equation 2.2, the permeate flux was calculated by measuring the quantity of permeate collected during a certain time and dividing it by the effective membrane area for filtration (Li *et al.*, 2006).

$$\begin{aligned} \text{Permeate flux, } J \\ = \frac{\text{permeate volume}}{\text{membrane area} \times \text{time}} (\text{L m}^{-2} \text{ h}^{-1}) \end{aligned} \quad (\text{Equation 2.2})$$

Cross flow ultrafiltration has been used to separate microbial cells and protein from fermentation broths (Li *et al.*, 2006). At the initial stage of cross flow filtration the yeast cells and other particles were deposited on the membrane to form a cake similar to dead-end filtration. The flux through the ultrafiltration membrane rapidly decreased in

the first 15 minutes of filtration and then steady state was achieved after the initial microbial cake was deposited on the membrane.

### **2.6.3 Nanofiltration**

Nanofiltration (NF) refers to a filtration process with a membrane MWCO of 300 to 1,000. For such membranes, the MWCO falls in the separation domain situated between reverse osmosis and ultrafiltration. Unlike reverse osmosis, the retention of salts in nanofiltration is low for molecular weight below 100; it is high for organic molecules of molecular weight above 300 (Affleck, 2000).

Nanofiltration membranes have been commercially manufactured. Nanofiltration membranes are capable of concentrating sugars, divalent salts, bacteria, proteins, particles, dyes, and other particles with molecular weight greater than 1000. Nanofiltration membranes reject molecules based on size when the particles are too large to pass through the pores. In addition, nanofiltration membranes can also use charge to reject molecules, much like reverse osmosis (Affleck, 2000).

The most promising application for nanofiltration is purification of ground water and surface water. This process is applied to retain micro-pollutants such as herbicides, and insecticides. Generally, the retention of low molar mass organics in the range of 200 to 1000 g/mol, and multivalent salts such as calcium salts can be achieved by NF. The driving pressure that usually applied in NF processes is in the range 3- 20 bars. The industrial applications of NF are the concentration of product streams with specific components such as proteins, enzymes, antibiotics and dyes. NF is also used to separate low molar mass solutes such as inorganic salts or small organic molecules such as glucose, and sucrose from a solvent. NF membranes can be used for softening the hard water (Mohammad, 2008).

#### 2.6.4 Reverse Osmosis

Reverse osmosis (RO) is the process of forcing water through a membrane from a more concentrated to less concentrated aqueous solution. Reverse osmosis utilizes extremely fine pores in the membranes that are typically made from cellulose acetate. The pores are believed to be less than 0.001  $\mu\text{m}$  in diameter. However, reverse osmosis is not filtration. Filtration is the removal of particles by size exclusion or the particles are too large to go through physical pores. In the case of reverse osmosis, such pores have never been viewed with a microscope. It is more likely that the small molecules permeate the reverse osmosis membrane by diffusive forces (Affleck, 2000).

The retention of all low molar mass solutes can be achieved by RO. The RO membranes are used in desalination of seawater. High potable water recovery can be obtained from seawater in single stage operation. Since the osmotic pressure increases in the retentate side, high applied pressure ranging from 20-100 bars is required. The average hydrodynamic pressure in the seawater desalination process is about 60 bars. This pressure can be enough to exceed the osmotic pressure of seawater that is around 25 bars (Mohammad, 2008).

Retention of low molar mass solvents such as methanol and ethanol is fairly good by RO. However, the rejection of the solutes by RO strongly depends on the type of the membrane. The main industrial applications of the RO are production of ultra-pure water for electronic industry, concentration of fruit juice and sugars in food industry, and concentration of milk in dairy industry (Mohammad, 2008).

Both asymmetric and composite membranes are used for RO. The structure of the latter membranes is denser than NF membranes. The top layer is formed by interfacial polymerization reaction. Polysulfone or polyethersulfone, cellulose triacetate and aromatic polyamides are usually used to form support layer of the RO membrane (Mohammad, 2008).

## 2.7 Membrane Fouling

Fouling is a complex phenomenon which cannot be totally avoided. It originates from the combined effects of different factors on the membrane: process conditions, process water content, and membrane characteristics. Membrane fouling can result in a flux decline, a decreased life of membrane modules and an increase in operating cost. In addition, membrane fouling reduces the production rate and increase the complexity of membrane performance (Sakinah *et al.*, 2007). Therefore it has been recognized as the biggest obstacle to membrane filtration in practice.

Membrane fouling is classified into two categories namely reversible and irreversible membrane fouling. Reversible membrane fouling can be removed by physical cleaning such as hydraulic backwashing. Another one is an irreversible membrane fouling which cannot be removed by physical cleaning but can be removed by chemical cleaning (Hashino *et al.*, 2010).

Many studies have been carried out to understand and control membrane fouling. Puro *et al.*, (2010) has stated that the easiest way to optimize the filtration process to ensure a low-fouling process is to choose an optimal membrane for filtration. Otherwise, the major membrane characteristics that affect fouling are charge, morphology and hydrophilicity. To solve this problem, a great deal of anti-fouling studies, such as blending, coating, adsorption, chemical-grafting, and radiation induced grafting, have been invented to modify the membrane (Liang *et al.*, 2010).

However, there are also studies on the operating and process conditions to control the membrane fouling such as solution pH, solution concentration, ionic strength, stirring speed, transmembrane pressure, cross flow velocity, temperature, etc. Among all the operating parameters, the transmembrane pressure and cross flow velocity are the most important parameters that influence to control the membrane fouling.

### 2.7.1 Effect of Cross Flow Velocity (CFV)

Studies have been conducted by several researches to reduce the fouling on membrane during the separation process. Cross flow velocity is used to reduce the effect of additional resistance due to concentration polarization and fouling or gel layer on the membrane surface (Mohammad, 2008). The influence of the concentration polarization and fouling in microfiltration might cause a dramatic permeate flux decline comparing with pure water flux.

Hwang and Sz, (2010) has been studied on the operating condition on the filtration flux for solute rejection and membrane fouling in BSA/dextran binary suspension cross-flow microfiltration. The filtration flux was increased 30–50% by increasing the cross-flow velocity or transmembrane pressure.

Besides that, cross flow velocity also influence on the formation of fouling layer during microfiltration and ultrafiltration during biological suspension (Choi *et al.*, 2005). The formation of a reversible fouling layer was actually prevented by a cross-flow velocity of 3.0 m/s for microfiltration membrane and 2.0 m/s for ultrafiltration membrane.

Fouling and regeneration of ceramic membranes used in recovering titanium silicalite-1 catalysts has been studied (Zhong *et al.*, 2007). Estimation of hydrodynamic forces acting on a single particle shows cross flow velocity (CFV) has an important effect on the deposition of TS-1 particles. However, after particles have deposited, increasing CFV will not resuspend them due to the strong and dense cake layer formation.

### 2.7.2 Effect of Transmembrane Pressure (TMP)

Transmembrane pressure has also been studied as operating parameter to measure and control the membrane fouling. Research on the separation of proteins from an aqueous solution by dead end filtration has been conducted to determine the effect of solution pH, initial protein concentration, transmembrane pressure, ionic strength and stirring speed (Lin *et al.*, 2008). Effective separation was achieved at a lower protein concentration, a lower TMP or a lower pH.

Thomassen *et al.*, (2005) has studied the fouling propensity during cross flow filtration of a model beer, primarily composed of dextrin and protein. An increase in transmembrane pressure resulted in a reduction in transmission of both the BSA protein and dextrin components of the model beer for a given cross flow velocity while an increase in cross flow velocity led to increased transmission of both the BSA and dextrin through the membrane for a given transmembrane pressure.

Otherwise, the permeate flux of both ceramic and polyvinylidene difluoride (PVDF) ultrafiltration membranes decreased with filtration time until it reached steady-state values (Ahmad *et al.*, 2005).

## 2.8 Membrane Cleaning

Membrane cleaning is performed due to the occurrence of fouling either reversible or irreversible. Reversible membrane fouling can be removed by physical cleaning such as hydraulic backwashing. Another one is an irreversible membrane fouling which cannot be removed by physical cleaning but can be removed by chemical cleaning (Hashino *et al.*, 2010).

Cleaning is usually performed in four forms either by physical, chemical, biological or enzymatic. Chemical cleaning means removing impurities by means of

chemical agents. Some of these cleaning agents are acid, alkali, surfactants, disinfectants and combined cleaning materials.

Most of the cleaning method is performed by using the chemical cleaning. Backwashing is applied mostly to neutralize back the membrane. Alkali-acid cleaning has been performed in cleaning the membrane during the filtration of cheese whey media (Li *et al.*, 2006). Besides, the membrane used was cleaned in ultrasonic cleaner with 0.1 M NaOH for approximately 30 min in the separation of protein by dead-end filtration (Lin *et al.*, 2008). The membrane was further cleaned by stored in the 0.05% sodium azide solution at 4°C.

Madaeni and Samieirad, (2010) were studied the use of acid, alkaline solution, surfactant and chelating agent on cleaning the membrane fouled in treatment of wastewater by reverse osmosis. They found that the acids were not effective in recovering the flux however, the two stages of caustic and detergent. Cleaning agents such as NaOH-SDS followed by acidic agent such as HCl provided high effective membrane regeneration.

There is also a study on membrane cleaning using electric pulse with an automated rig on the membrane surface (Ahmad *et al.*, 2002). The automated rig developed was proven to reduce the membrane fouling using electric pulse for both dead-end microfiltration and ultrafiltration processes. As the pulse duration and applied voltage increased, the average flux was also increased.

Furthermore, two types of chemical cleaning which are 0.1 M NaOH and 0.1 M HCl were applied as to determine the solutions effectiveness during the cyclodextrin separation (Sakinah *et al.*, 2007). The alkaline solution cleaning shows a higher removal of weak adsorption, which was about 11% more compared to the acidic solution cleaning. The dominant foulant was an organic element, which can be significantly removed effectively by alkaline cleaning rather than acidic cleaning.

## 2.9 Response Surface Methodology (RSM)

Response Surface Methodology (RSM) is used in optimizing the conditions of tested variables in maximizing the response of an experiment. Many reports revealed by using RSM, the response is maximized. Beside, the period of research also decreased. In other ways, RSM helps in saving time and money.

In the factorial design of experiments, when responses and input variable factors (e.g., the cross flow velocity and transmembrane pressure) are continuous, it is very useful to consider the factor response relationship in terms of a mathematical model such as the response function. For qualitative factors where there is no continuous link between the response and the levels of a factor, it is necessary to consider a comparison of the response between two levels of a qualitative factor. The factorial approach results in a considerable saving of time and materials devoted to the experiments (Lin *et al.*, 2008).

First, the factor that is independent of all simple effects of a factor is equal to its main effect. The consequences of variations in the factors and the main effects are the only quantities that need to be stated. Second, each main effect in factorial experiments is estimated with the same accuracy as if the whole experiment had been devoted to the factor alone. Thus, the advantages of this methodology contain (i) all experimental units are used in evaluating effects, resulting in the most efficient use of resources, (ii) the effects are evaluated over a wider range of conditions with the minimum of resources, and (iii) a factorial set of treatments is optimized for estimating main effects and interactions (Lin *et al.*, 2008).

In general, the linear terms are more significant than the quadratic interactions. Results show that TMP and initial protein concentration are the most significant factors, and stirring speed is the less significant one in the present filtration process. It is noticed that the model parameters are determined by an ANOVA fitting exercise, so that the model could adequately describe most of the data (Lin *et al.*, 2008).

## CHAPTER 3

### METHODOLOGY

#### 3.1 General Methodology

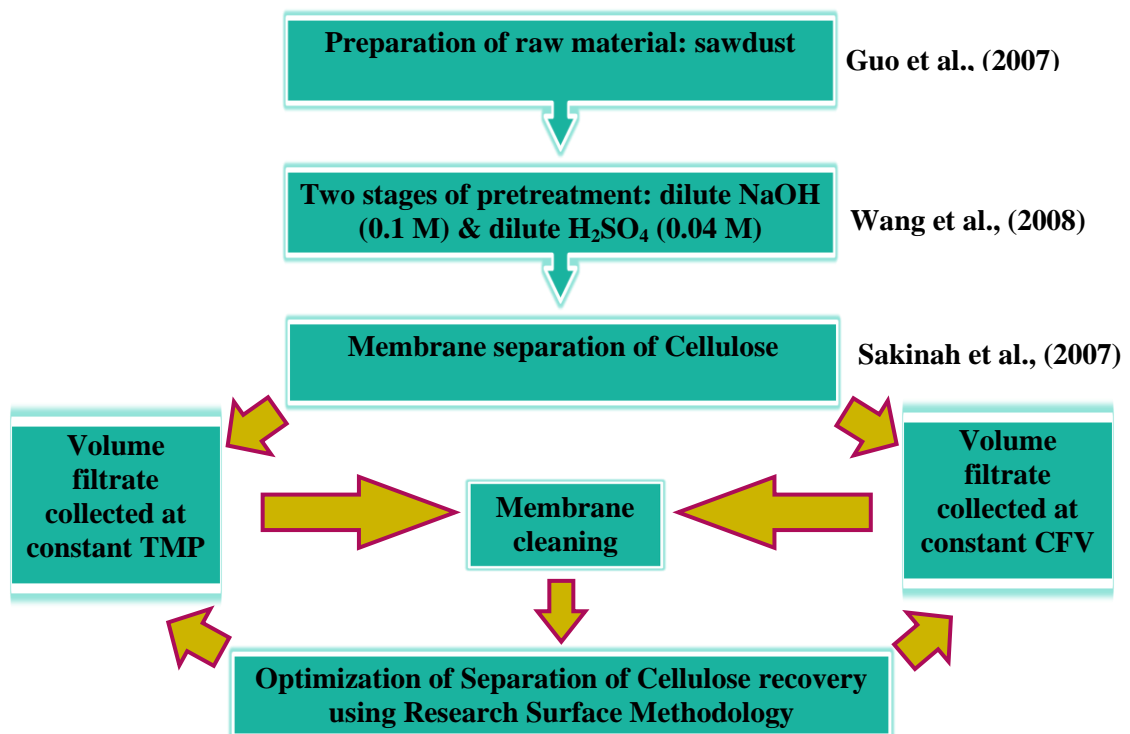


**Figure 3.1:** Process flow for recovery and separation of cellulose.

### 3.2 Preparation of Raw Material

Raw material used was hardwood sawdust (Keruing). Hardwood sawdust was taken from the saw mill factory at Gambang, Pahang (Figure 3.2). For the preparation of sawdust before pretreatment, 10 kg of sawdust was grind using the blender to reduce the particle size and surface area. Sawdust was then sieved using shack sieve with a pore size of 2 mm to provide fine size class of sawdust (Figure 3.3). After that sawdust was dried (Figure 3.4) in the oven at 60°C about 24 hours. Then it was stored in seal bags at room temperature until further process (Guo *et al*, 2007).



**Figure 3.2:** Sawdust taken from sawmill factory.



**Figure 3.3:** Sawdust after grinder and sieved.



**Figure 3.4:** Sawdust after drying.

### **3.3 Two-stage of Pretreatment Process**

#### **3.3.1 Sodium Hydroxide (NaOH) pretreatment**

100 L of 0.1M sodium hydroxide (NaOH) solution was prepared for the first pretreatment process. 400 g of NaOH (solid) was weight using analytical balance. After that, 400 g NaOH was dilute with distilled water in the 2000 mL volumetric flask until reach the meniscus line. The NaOH solution was stored in chemical cabinet until it used for the pretreatment. The solution will be added with 98 L of distilled water during the pretreatment process.

For sodium hydroxide (NaOH) pretreatment, 5 kg of sawdust was first weigh using electronic balance. Then the sawdust was introduced into the membrane reactor. The prepared NaOH solution was added with remaining 98 L of distilled water and filled into the membrane reactor. The solution mixture (sawdust and NaOH) was allowed to mix to react and was stirred at impeller speed of 15-20 rpm. The pretreatment was then performed inside the membrane reactor at 75 °C for 24 hours respectively (Figure 3.5).

After the pretreatment had finished, the sample was cool down at room temperature. The sample was then filtered using filter cloth to separate the solid residue and liquid. The liquid waste was stored in the waste tank while the solid residue was collected and stored before undergo further pretreatment process (Figure 3.6).



**Figure 3.5:** Sodium hydroxide (NaOH) pretreatment in membrane reactor.



**Figure 3.6:** Sawdust (solid residue) after pretreatment process.

### 3.3.2 Sulfuric Acid (H<sub>2</sub>SO<sub>4</sub>) pretreatment

100 L of 0.04M H<sub>2</sub>SO<sub>4</sub> solution was prepared. The solution was prepared by diluted the 220 mL of acid with 100L of distilled water. First of all, 220 mL of sulfuric acid was measured and then was filled into 2000 mL volumetric flask. Distilled water was added until it reached the meniscus line. The solution was stored before being used for pretreatment process. The solution will be further added with 98 L of distilled water during the pretreatment process.

For sulfuric acid (H<sub>2</sub>SO<sub>4</sub>) pretreatment, the remaining sawdust residue approximately 5 kg from NaOH pretreatment was first introduced into the membrane reactor (Figure 3.7). The prepared H<sub>2</sub>SO<sub>4</sub> solution was added with remaining 98 L of distilled water and filled into the membrane reactor. The solution mixture (sawdust and H<sub>2</sub>SO<sub>4</sub>) was allowed to mix to react and was stirred at impeller speed of 15-20 rpm. The pretreatment was then performed inside the membrane reactor at 75°C for 24 hours respectively (Figure 3.8). After finished with the pretreatment, the sample was cooled at certain temperature before undergo membrane filtration process.



**Figure 3.7:** Pretreated sawdust (NaOH pretreatment) being introduced into membrane reactor.



**Figure 3.8:** Sulfuric acid ( $\text{H}_2\text{SO}_4$ ) pretreatment in membrane reactor.

### 3.4 Membrane Separation of Cellulose

Membrane reactor system consists of membrane module, peristaltic pump, flow meter and pressure gauge (Figure 3.9) was used for membrane filtration process. Submerged filter membrane was used during the experiment. The material of the membrane used was ceramic membrane with pore size of  $0.9 \mu\text{m}$  and effective membrane area of approximately  $0.03 \text{ m}^2$ . The submerged membrane was horizontally assembled inside the membrane reactor. The membrane reactor consists of a stainless steel vessel with a mechanical stirrer attached (Sakinah *et al.*, 2007). The mixing intensity of the process is 15-20 rpm.

The membrane filtration of the solution mixture from dilute  $\text{H}_2\text{SO}_4$  was performed. The process condition was at  $50^\circ\text{C}$  with impeller speed of 15-20 rpm to enhance the separation process and to avoid fast membrane fouled. The membrane filtration was performed at different transmembrane pressure (TMP) ranging from 0.5 to

2.5 bar and cross flow velocity ranging from 0.2 to 0.18 m/s respectively. Volume of permeate was collected for every 5 minutes for 60 minutes. The permeate flux was calculated using Equation 3.1 by measuring the quantity of permeate collected during a certain time and dividing it by the effective membrane area for filtration (Li *et al.*, 2006).

$$\begin{aligned} \text{Permeate flux, } J \\ = \frac{\text{permeate volume}}{\text{membrane area} \times \text{time}} \text{ (L m}^{-2} \text{ h}^{-1}) \end{aligned} \quad \text{(Equation 3.1)}$$

The volume of permeate collected for every 5 minutes as shown in Figure 3.10. The operating parameters to study the flux decline on the ceramic membrane were divided into two parts. First, the TMP was kept constant at 1 bar while the cross flow velocity varied at 0.02, 0.06, 0.10, 0.14 and 0.18 m/s. In the second part, the cross flow velocity was kept constant at 0.06 m/s and the TMP varied at 0.5, 1.0, 1.5, 2.0 and 2.5 bars. All experiments were conducted at a constant temperature of 50°C. These experiments were repeated twice and the average values were recorded.



**Figure 3.9:** Membrane reactor system.



**Figure 3.10:** Parameter adjustment and product collection.

### 3.5 Membrane Cleaning

After each experiment, cleaning of the membrane was performed. This is because after filtration process, membrane performance will be reduced to certain level. Membrane appearance is shown in Figure 3.11 (a) before and (b) after filtration process. Figure 3.12 and Figure 3.13 shows the cleaning process involved backwashing with water and chemical cleaning with 0.05M NaOH solution. The first approach used where the membrane was flushed with water for about 5 to 10 minutes. Another approach by chemical cleaning was by soaked the membrane in 0.05M NaOH solution for overnight. The membrane was rinsed with water for several times before continue with the next experiment.



**Figure 3.11:** Membrane appearance and sample (a) before and (b) after filtration process.



**Figure 3.12:** Backwashing using water.



**Figure 3.13:** Chemical cleaning using 0.05M NaOH

### 3.6 Optimization of Separation of Cellulose Recovery using Response Surface Methodology.

The optimization was done by using the Response Surface Methodology (RSM). The low values and high values from each parameter were selected from the screening process. There were 17 experiments that were designed by RSM which need to be carried out. Table 3.1 shows the values that were used during optimization in RSM.

**Table 3.1:** Low and high values for optimization in Response Surface Methodology

Experimental range and levels of independent variables		
Variables	Range and levels	
	Low	High
Transmembrane pressure (bar)	1	2.5
Cross flow velocity (m/s)	0.06	0.14

## **CHAPTER 4**

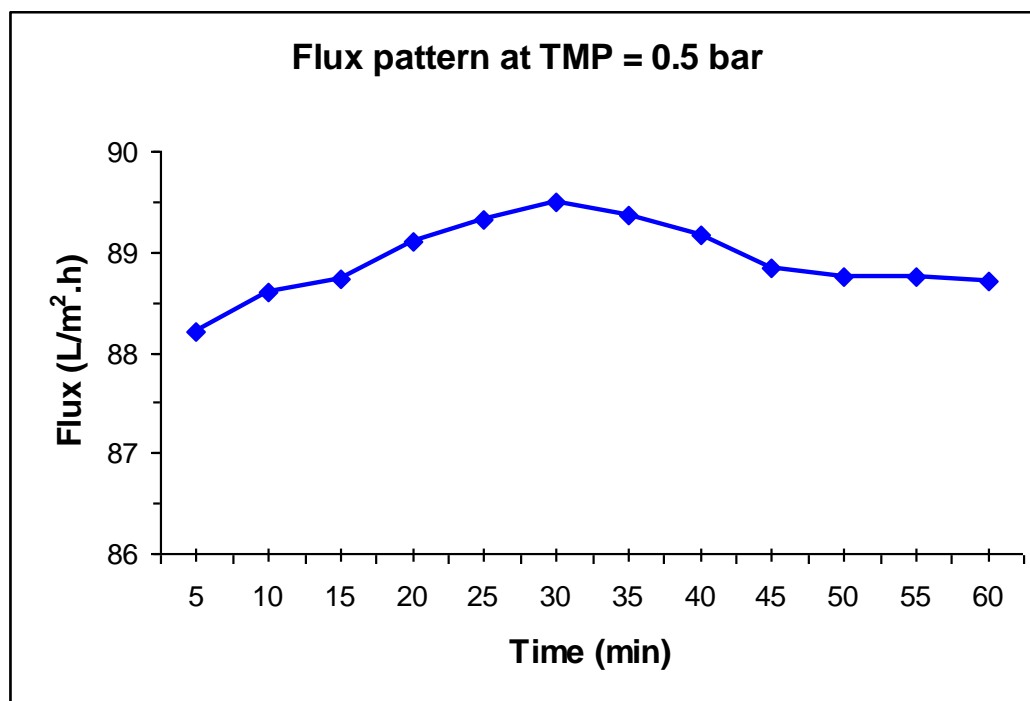
### **RESULT AND DISCUSSION**

#### **4.1 Introduction**

In this chapter, the results obtained from the experiment were discussed. The experiment was performed to study the effect of transmembrane pressure (TMP) and cross flow velocity (CFV) on the permeate flux during the separation of cellulose recovery from sawdust wood hydrolysates. Besides that, the optimum TMP and CFV during membrane filtration was also studied. In order to achieve the objectives, the experiment was continued to the optimization of the separation of cellulose recovery using Response Surface Methodology (RSM).

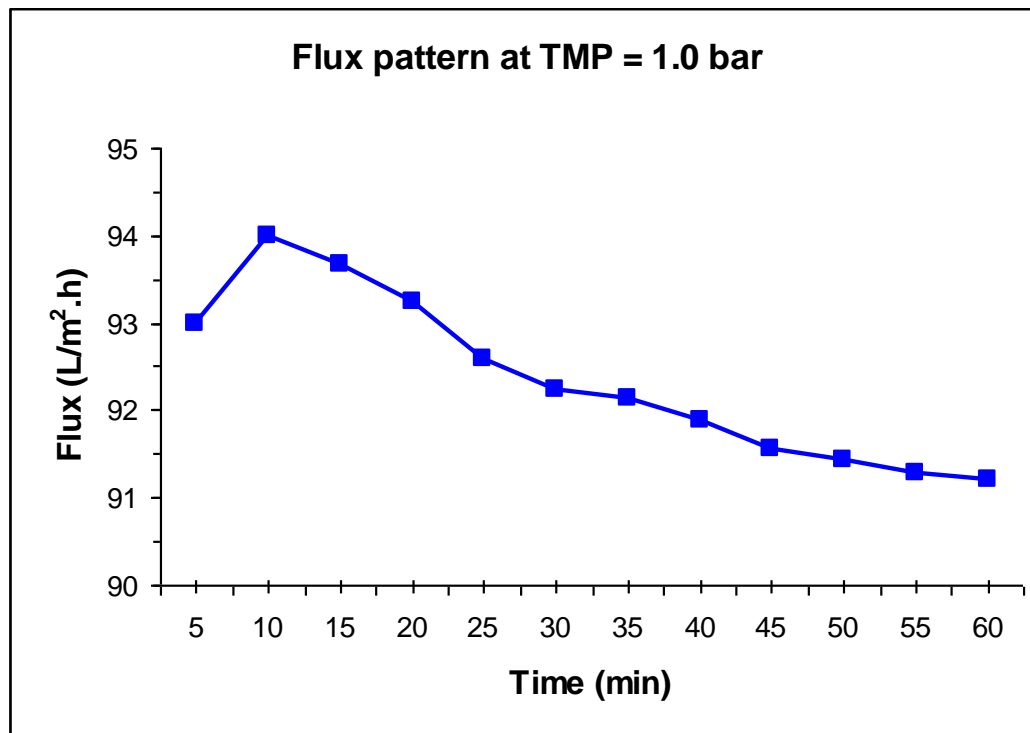
#### **4.2 Effect of Transmembrane Pressure (TMP) on Flux**

In order to study the permeate flux decline, the experiment was performed at various transmembrane pressures (TMP) which values are at 0.5, 1.0, 1.5, 2.0 to 2.5 bars. The other variable which is cross flow velocity (CFV) was kept constant at 0.06 m/s in order to get the actual nature of dependence. The separation process was performed at 60 minutes duration at a temperature of 50 °C.



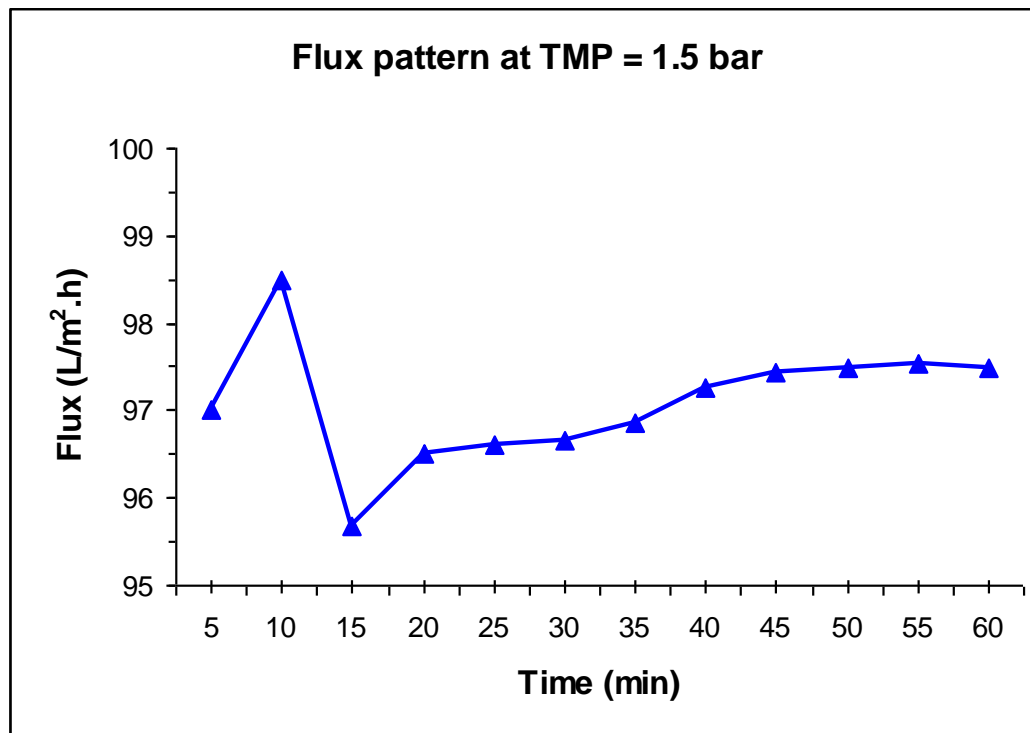
**Figure 4.1:** Flux pattern at TMP of 0.5 bar.

Figure 4.1 shows the change in permeate flux over time under TMP of 0.5 bar. The plotted pattern shows that the permeate flux was increased for the first 30 minutes and later on decreased before achieved the steady state flux at the last 15 minutes. The permeate flux was increased for about 8.94% when the retention time is increased. The flux was increase due to the unstable flow rate of the permeate that flow through the flow meter and also the pressure gauge reading that are not constant at 0.5 bar.



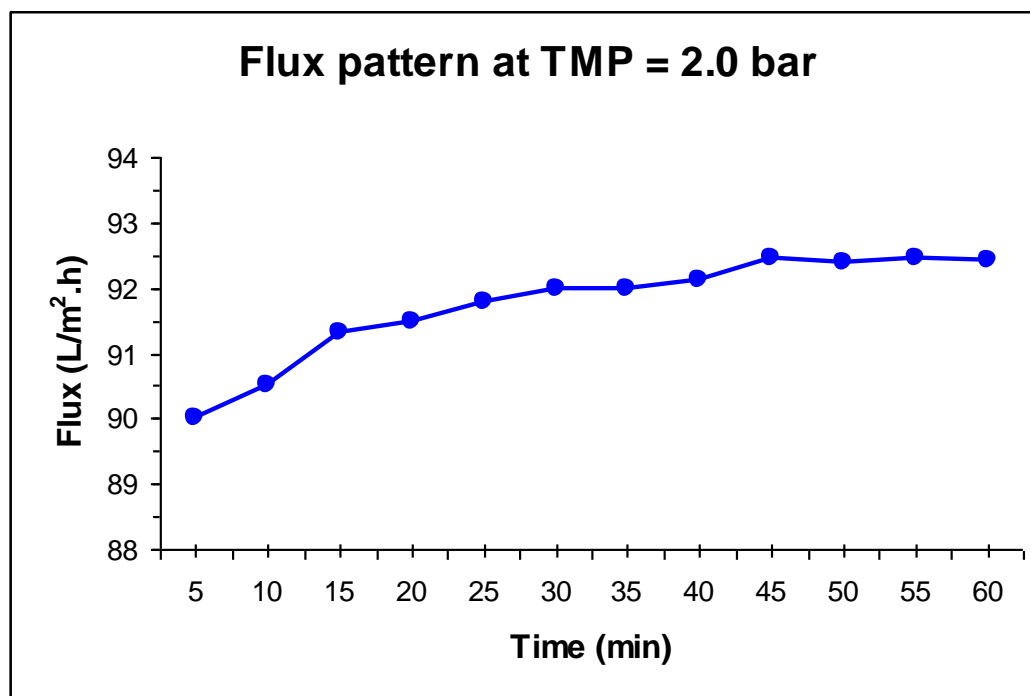
**Figure 4.2:** Flux pattern at TMP of 1.0 bar.

Behavior on the permeate flux at TMP of 1.0 bar is shown in Figure 4.2. The plotted pattern shows that the flux was increase at the first 10 minutes. Later on, the flux was decreased linearly until it reaches the steady state condition at last 10 minutes. This shows that the flux was decreased to 2.68% when the operating time is increased. The decrease of the flux over time is a result of fouling of the membranes (Li et al., 2006).



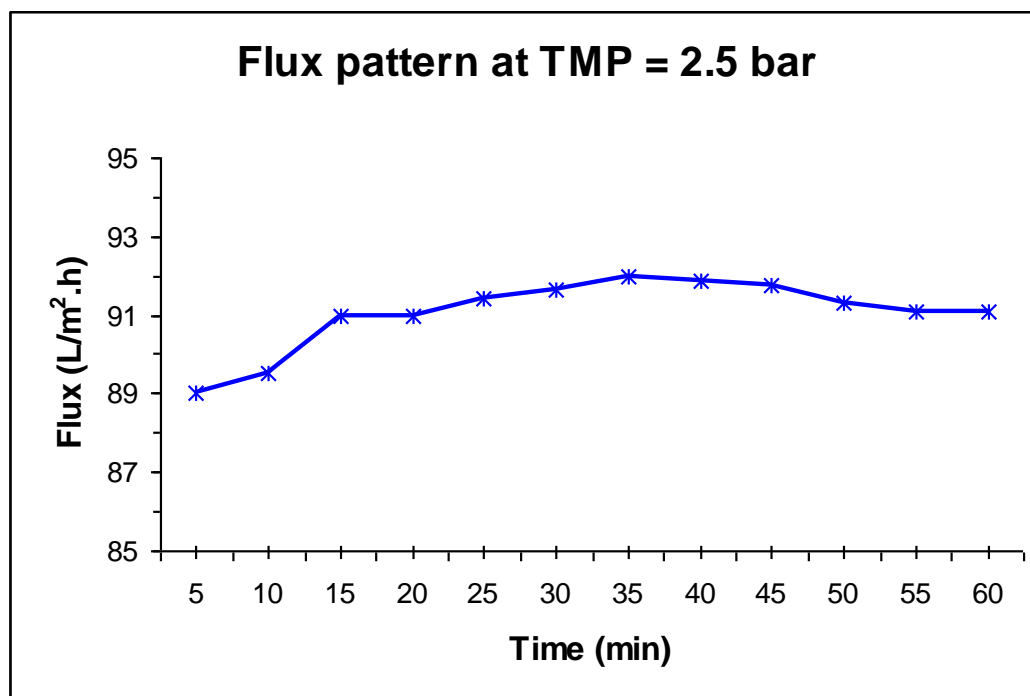
**Figure 4.3:** Flux pattern at TMP of 1.5 bars.

Figure 4.3 shows the change in permeate flux over time at TMP of 1.5 bars. The plotted pattern shows that the permeate flux was increase at the first 10 minutes, decrease at the next 5 minutes before continued increased until it reaches the steady state at last 15 minutes. The flux was increased to 0.22% when the operating time increased. The flux behavior was not consistent. This is because the operating condition is not stable and fluctuate during the experiment such as the permeate flow rate and the applied pressure which were not constant.



**Figure 4.4:** Flux pattern at TMP of 2.0 bars.

From Figure 4.4, the flux pattern was obtained at the TMP of 2.0 bars. The pattern shows that the flux was increase almost linearly over time. The increment of flux is linear until it reaches the steady state at the last 20 minutes. The flux was increased to 2.67% when the operating time increased. This was due to the fluctuated flow rate of the feed and unstable pressure gauge reading.



**Figure 4.5:** Flux pattern at TMP of 2.5 bars.

Flux decline at TMP of 2.5 bars is shown at Figure 4.5. The flux pattern was obtained where the flux increased until 40 minutes before decrease a little until achieved steady state at the last 10 minutes. The flux was increased for about 2.67% when increased in operating time. The flux was increases due to the unstable flow rate of permeate that flow through the membrane and the pressure gauge reading is not constant at 2.5 bars.

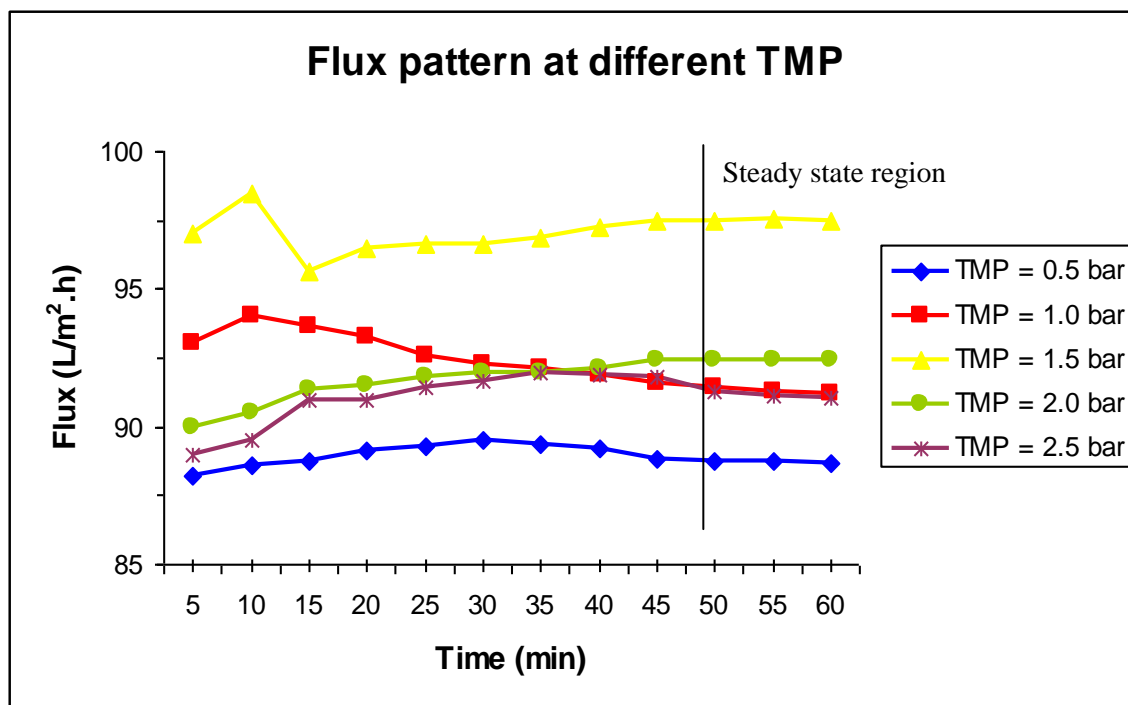


**Figure 4.6:** Comparison of permeate flux at different TMP.

Based on Figure 4.6, the flux behavior at different TMP was shown. The effect of transmembrane pressure on the permeate flux can be observed. Increased in transmembrane pressure caused an increase of the permeate flux. Beyond a certain pressure, the increase in permeate flux with pressure was negligible which indicates that there is an optimum pressure to obtain the maximum permeate flux. From this experiment, the highest flux was obtained at an optimum TMP of 1.5 bars with percentage of flux decline at 2.68%.

Similar results were also reported by Li *et al.*, (2006) who obtained the optimum pressure for maximum permeate flux during the separation of cells and proteins from fermentation broth using ultrafiltration. Another findings showed that the increased in transmembrane pressure was decreased the S/N ratio in the study of effect of operating conditions on membrane fouling in treatment of pulp and paper mill wastewater by nanofiltration (Gonder *et al.*, 2010). He added that in general, an increased in an applied transmembrane pressure could contribute to the membrane fouling which will result in increasing of osmotic pressure, and cause flux decline.

Besides that, similar phenomenon was also found by Babel and Takizawa, (2010) when treating algae-laden water using microfiltration. They found that the cake layer resistance which will result in fouling increases with the increase of TMP. No increase in resistance was found with pressure more than 30 kPa as the maximum level of compressibility was achieved.

### 4.3 Effect of Cross flow Velocity (CFV) on Flux

The flux decline was studied by performed the experiment at various cross flow velocity (CFV) which values are at 0.02, 0.06, 0.10, 0.14 and 0.18 m/s. The other variable which is transmembrane pressure (TMP) was kept constant at 1.0 bar in order to get the actual nature of dependence. The separation process was performed at 60 minutes duration at a temperature of 50 °C.

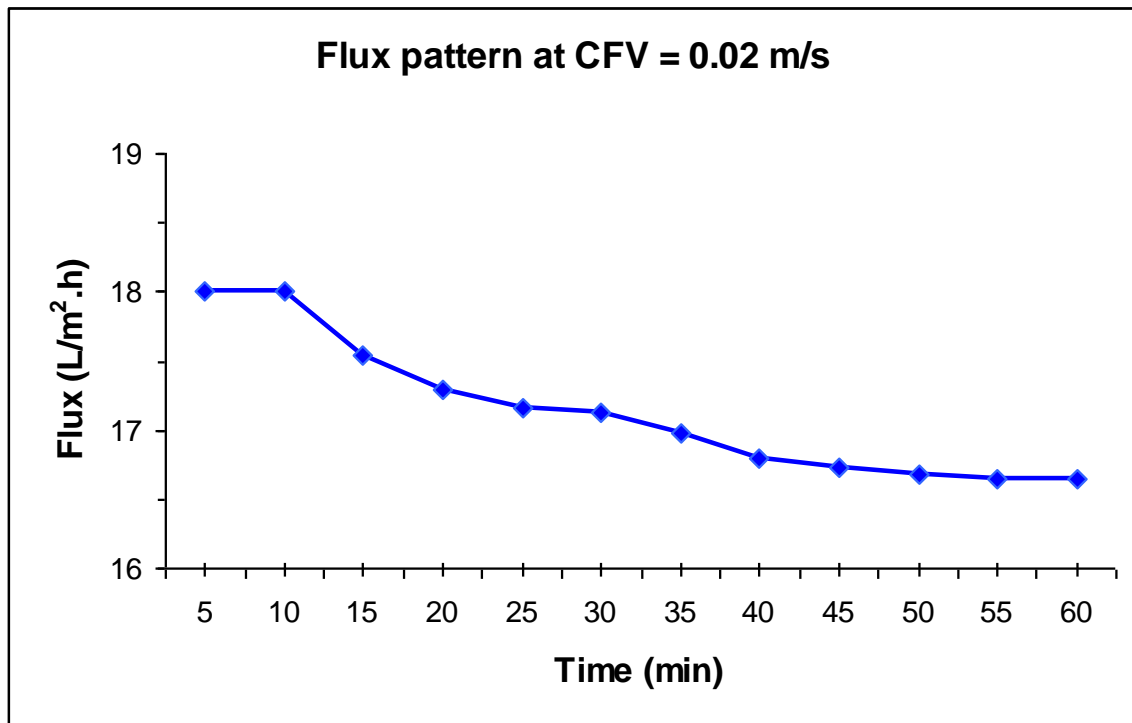
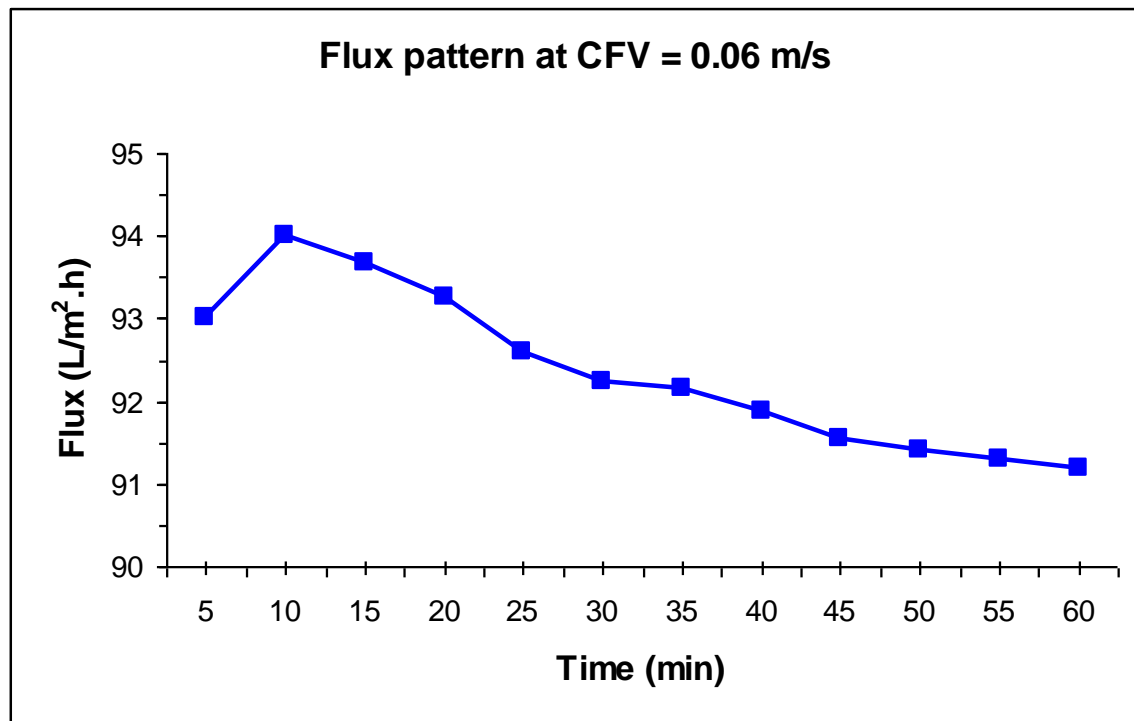


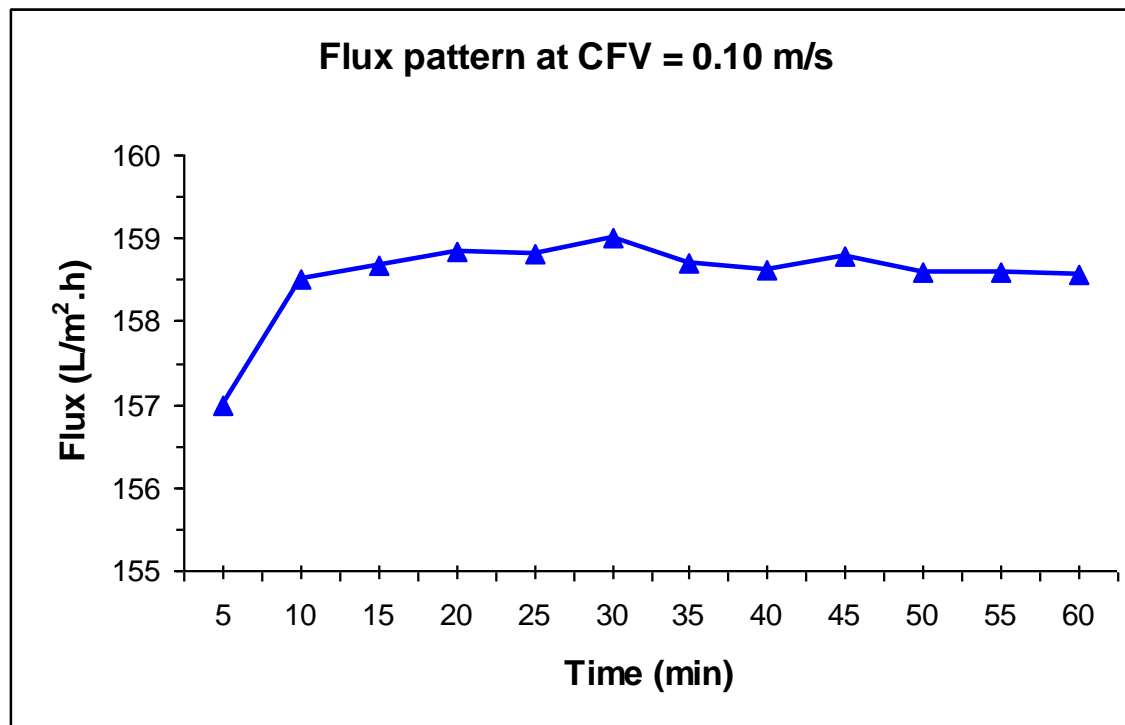
Figure 4.7: Flux pattern at CFV of 0.02 m/s.

Figure 4.7 shows the flux behavior at CFV of 0.02 m/s. From the graph, the flux was constant at the first 10 minutes. The flux then decreased almost linearly before achieved steady state. This shows that the overall flux was decreased around 6.95% when the operating time increased. This is because of the performance of filter membrane was reduced due to the fouling phenomenon.

The change in permeate flux over time at CFV of 0.06 m/s was shown in Figure 4.8. The plotted pattern shows that the permeate flux was increase at the first 10 minutes and then decrease until it reaches the steady state at last 10 minutes. The flux was decreased to 2.13% when the operating time increased. This shows the flux decrease happen due to the formation of cake layer on the membrane surface proportional to the operating time.



**Figure 4.8:** Flux pattern at CFV of 0.06 m/s.



**Figure 4.9:** Flux pattern at CFV of 0.10 m/s.

Behavior on the permeate flux at TMP of 0.10 m/s is shown in Figure 4.9. The plotted pattern shows that the permeate flux was increase rapidly at the first 10 minutes before increase gradually until it reaches the steady state condition at last 15 minutes. This shows that the flux was increased to 1.26% when the operating time is increased. This is because the flow rate of the feed through the membrane was unstable and also due to the leaking on the membrane fitting through the permeate line.

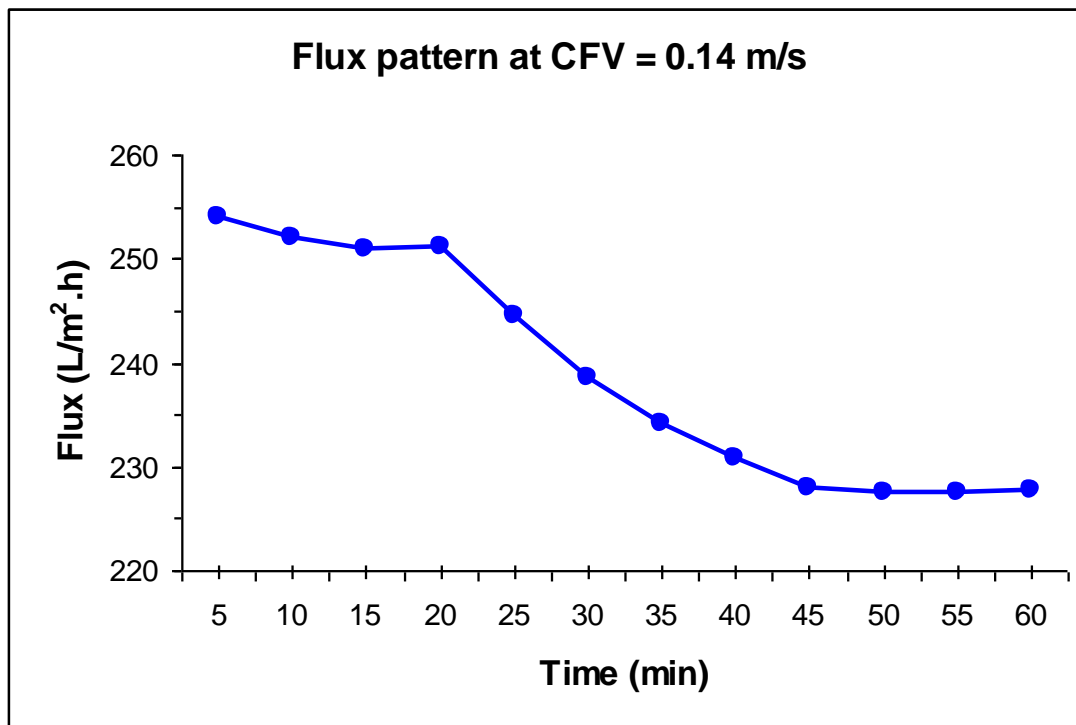


**Figure 4.10:** Flux decline at CFV of 0.14 m/s.

Flux behavior at CFV of 0.14 m/s is shown at Figure 4.10. The flux pattern was obtained where the flux decreased gradually before decreased linearly until achieved steady state at last 20 minutes. The flux was decreased for about 11.75% when increased in operating time.

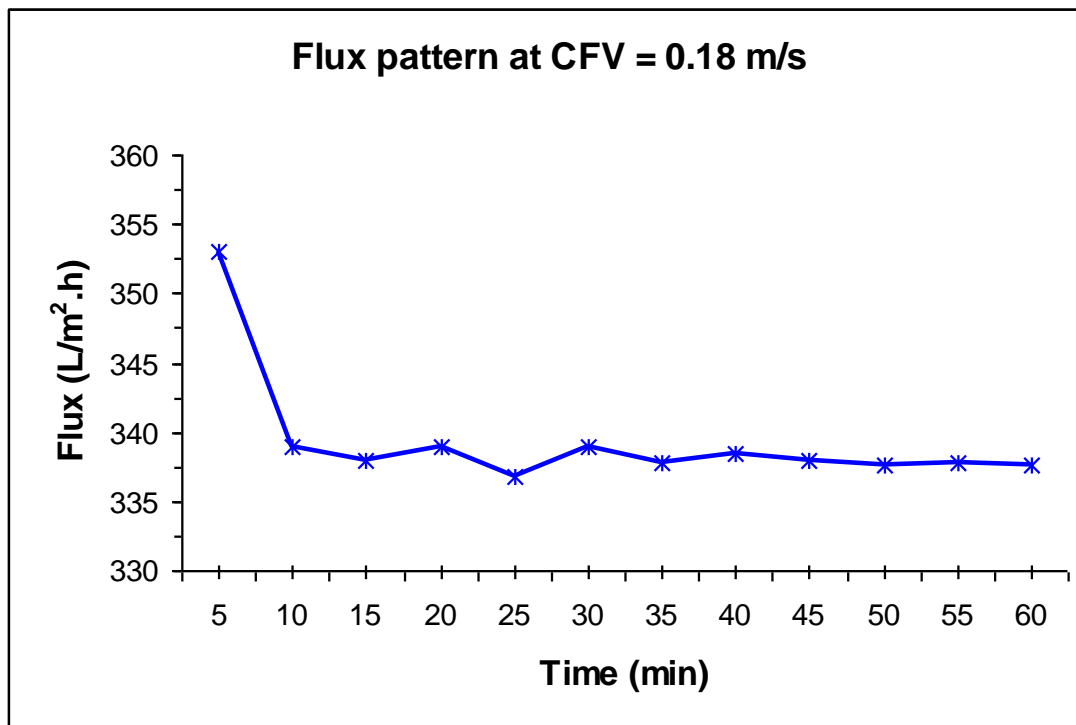


**Figure 4.11:** Flux pattern at CFV of 0.18 m/s.

Figure 4.11 shows the flux decline at CFV of 0.06 m/s. The plotted pattern shows that the permeate flux was decreased rapidly at the first 10 minutes and then decrease gradually until it reaches the steady state at last 15 minutes. The flux was decreased to 4.61% when the operating time increased. The rapid decrease in flux shows that the membrane has fouled at the earlier stage due to the cake formation on the membrane surface.

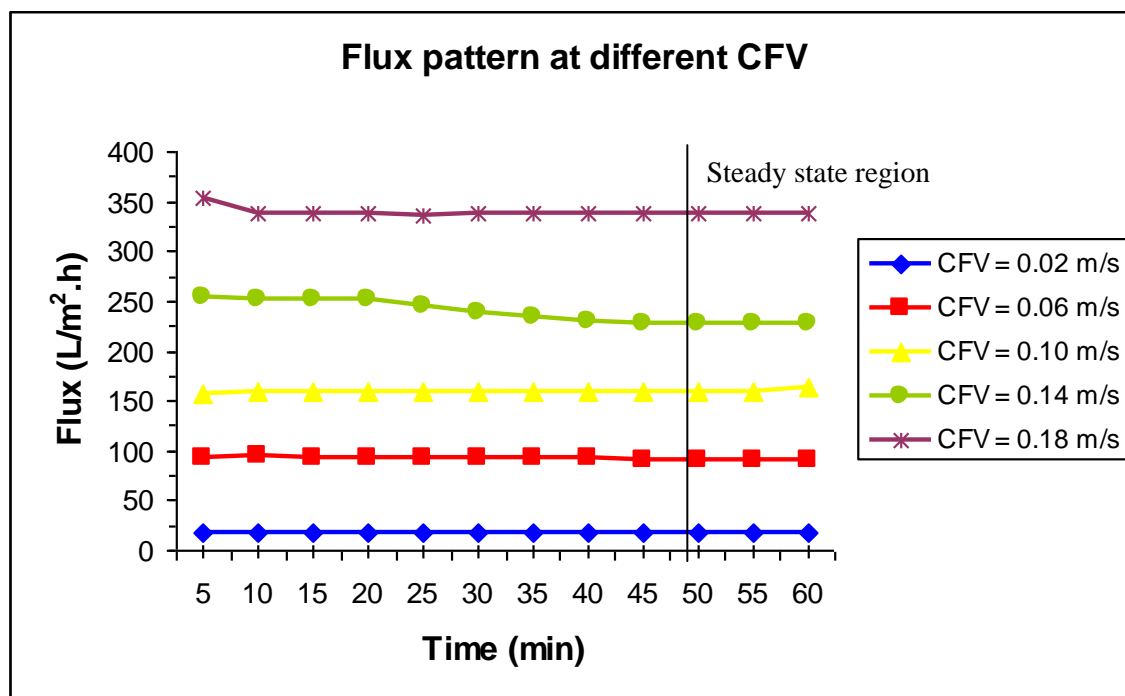


**Figure 4.12:** Comparison of permeate flux at different CFV.

Based on Figure 4.12, the effect of cross flow velocity on the permeate flux can be observed. It is evident that an increase of cross-flow velocity caused a higher permeate flux. The decrease in permeate flux over time is a result of fouling of the membranes. Increasing the cross-flow velocity also resulted in an increase of the permeate flow rate linearly (Choi *et al.*, 2005). From this experiment, it was found that the highest flux declined was obtained at an optimum CFV of 0.14 m/s with percentage of flux decline at 11.75%.

This result are in agreement with the findings of Zhong *et al.*, (2007) who reported that the hydrodynamic forces acting on a single particle shows CFV has an important effect on the deposition of titanium salicilate-1 particles on ceramic membrane during ultrafiltration. However, after particles have deposited, increasing CFV will not resuspend them due to the strong and dense cake layer formation.

Besides that, a significant flux decline was clearly observed during the treatment of palm oil mill effluent (POME) in both ceramic and polyvinylidene difluoride (PVDF) membranes where the reduction percentage is within 50-60% (Ahmad *et al.*, 2005). A rapid flux decline was observed in the ceramic membrane compared to the PVDF membrane whereby only within less than 10 min a plateau was reached for the ceramic membrane.

#### **4.4 Optimization of Separation of Cellulose Recovery using Response Surface Methodology**

The main objective of the response surface methodology (RSM) is to determine the optimum operating conditions for the system and also to optimize the response based on the factors investigated (Idris *et al.*, 2006). In this study, parameter of transmembrane pressure (TMP) and cross flow velocity (CFV) were selected for RSM and central composite design (CCD) was applied to identify the optimum TMP and CFV in order to maximize the permeate flux.

The response surface design developed is based on central composite design (CCD) whereby the factorial portion is a full factorial design with all combinations of the factors at two levels (high, +1 and low, -1 levels), the centre points (coded level 0), which is the midpoint between the high and low levels, is repeated thrice, the axial or star points for which all but one factor is set at 0 and the one factor is set at the outer value corresponding to an  $\alpha$  value of 2. The experimental plan generated using the Design Expert Version 6.0 software is shown in Table 4.1. The design involves 17 experimental runs and the response variables measured was the flux.

**Table 4.1:** Design layout and experimental results

Standard Run no.	Run	Block	Factors			Response
			TMP: bar (A)	CFV: m/s (B)	Time: min (C)	Flux (L/m <sup>2</sup> .h)
1	15	1	1.00	0.06	20.0	92.50
2	17	1	2.50	0.06	20.0	89.50
3	5	1	1.00	0.14	20.0	251.50
4	12	1	2.50	0.14	20.0	213.50
5	11	1	1.00	0.06	45.0	90.67
6	4	1	2.50	0.06	45.0	91.33
7	3	1	1.00	0.14	45.0	212.44
8	1	1	2.50	0.14	45.0	165.11
9	8	1	0.25	0.10	32.5	168.31
10	9	1	3.25	0.10	32.5	153.54
11	16	1	1.75	0.02	32.5	29.23
12	2	1	1.75	0.18	32.5	260.00
13	6	1	1.75	0.10	7.5	164.00
14	7	1	1.75	0.10	57.5	157.39
15	10	1	1.75	0.10	32.5	163.08
16	13	1	1.75	0.10	32.5	160.62
17	14	1	1.75	0.10	32.5	158.46

The levels of flux at each experimental point using are given in Table 4.1. Table 4.1 showed that Standard order no. 12 gave the highest permeate flux with 260 L/m<sup>2</sup>.h. The operating parameter of Standard no. 12 was 1.75 bar and 0.18 m/s. The lowest permeate flux was 29.23 L/m<sup>2</sup>.h which was detected at Standard order no. 11 with the operating parameter were 1.75 bar and 0.02 m/s.

The permeate flux results were input into the Design Expert software for further analysis. Examination of the Fit Summary output revealed that the quadratic model is statistically significant for the flux rate. Therefore, this model was used to represent the responses for further analysis.

#### 4.4.1 ANOVA Analysis

Analysis of variance (ANOVA) was used as an appropriate to the experimental design to analyze the results. The full quadratic second-order polynomial equation was found to explain the flux by applying multiple regression analysis on the experimental data. All terms regardless of their significance were included in the equation in term of coded factor and actual factor.

The final empirical model in terms of coded factors was presented as follows:

$$\begin{aligned} \text{Flux} = & +158.09 - 7.33A + 58.76B - 6.29C - 4.15B^2 - 10.37AB \\ & - 10.93BC \end{aligned} \quad (\text{Equation 4.1})$$

where Flux is the predicted response, A is the coded value of TMP; B is the coded value of CFV and C is the coded value for time. This equation consists of 1 offset, 3 linear, 1 quadratic and 2 interaction.

In terms of actual factors the final empirical models are as follows:

$$\begin{aligned} \text{Flux} = & -112.85192 + 24.81167\text{TMP} + 3303.39279\text{CFV} + 1.68290\text{Time} \\ & - 2594.17748\text{CFV}^2 - 345.79167 (\text{TMP})(\text{CFV}) \\ & - 21.86250(\text{CFV})(\text{Time}) \end{aligned} \quad (\text{Equation 4.2})$$

The coefficient values of Equation 4.1 were calculated using Design Expert Software and *P*-value of every term and the interaction are listed in Table 4.2 Based on Table 4.2, the linear term of TMP (A), linear term of CFV (B), linear term of Time (C) squared terms of CFV( $B^2$ ), interaction term of TMP and CFV (AB) and interaction term of CFV and Time (BC) are significant model terms that influence the flux due to the *P*-value less than 0.05.

**Table 4.2:** Regression coefficient and P- value calculated from the model

Variables	Coefficient	<i>P</i> -value <sup>a</sup> (Prob > F)
Offset	158.09	
A	7.33	0.0072
B	58.76	< 0.0001
C	6.29	0.0161
B <sup>2</sup>	4.15	0.0385
AB	10.37	0.0071
BC	10.93	0.0052

<sup>a</sup>Values of *P*-value less than 0.0500 indicate model terms are significant.

Table 4.3 and 4.4 show the ANOVA and regression analysis for the determination of permeate flux. The precision of a model is indicated by the determination coefficient ( $R^2$ ) and correlation coefficient ( $R$ ). The determination coefficient ( $R^2$ ) implies that the sample variation of 98.73% for determination of permeate flux was attributed to the independent variables tested. The  $R^2$  value also indicates that only 1.27% of the total variation was not explained by the model. The value of  $R$  (correlation coefficient) closer to 1 indicates the better correlation between the experimental and predicted values.

Here, the value of  $R$  (0.9936) for Equation 4.1 indicates a close agreement between the experimental results and the theoretical values predicted by the model equation. Meanwhile, the adjusted  $R^2$  (coefficient of determination) was calculated to be 97.97%, indicating that a good agreement existed between the experimental and predicted values of flux. The adequate precision value, which measured the signal to noise ratio is 42.087, which indicates an adequate signal. A ratio greater than 4 is desirable. Thus, this model can be used to navigate to the design space.

**Table 4.3:** ANOVA for response surface model

Model Terms	Values
R-Squared	0.9873
Adj R-Squared	0.9797
Pred R-Squared	0.9568
Adeq Precision	42.0866

Table 4.4 shows the *P*-values obtained were small, <0.0001 compared to a desired significance level, 0.05. This means the regression model was accurate in predicting the pattern of significance to the permeate flux.

**Table 4.4:** ANOVA table (partial sum of square) for quadratic model (response flux)

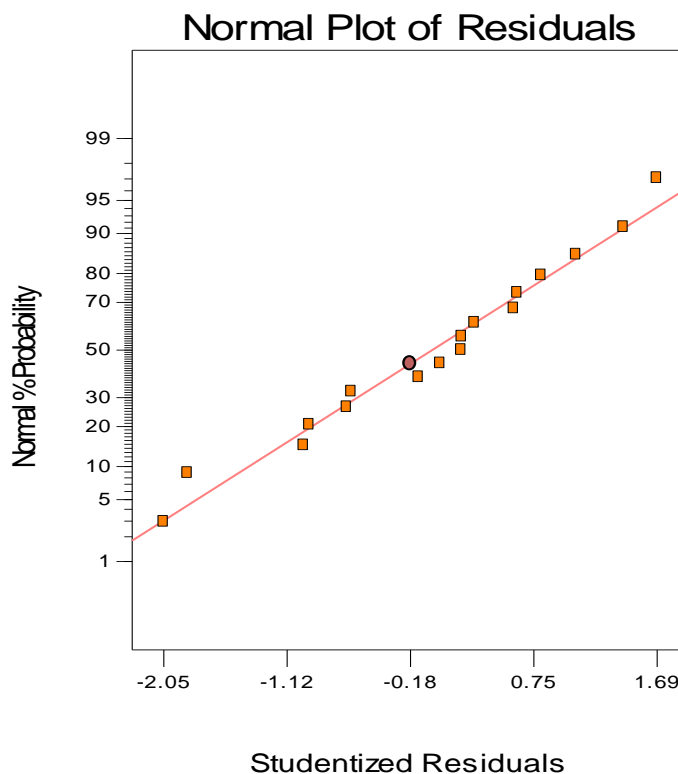
Source	Sum of Squares	DF	Mean Square	F Value	<i>P</i> Value (Prob > F)
Model	58974.1614	6	9829.0269	129.7866	< 0.0001
A	858.6365	1	858.6365	11.3378	0.0072
B	55235.5755	1	55235.5755	729.3536	< 0.0001
C	633.4031	1	633.4031	8.3637	0.0161
B <sup>2</sup>	429.6910	1	429.6910	5.6738	0.0385
AB	860.9175	1	860.9175	11.3679	0.0071
BC	955.9378	1	955.9378	12.6226	0.0052
Residual	757.3223	10	75.7322	-	-
Lack of Fit	746.6351	8	93.3294	17.4656	0.0553
Pure Error	10.6872	2	5.3436	-	-
Correlation Total	59731.4837	16	-	-	-

#### 4.4.2 Effect of Interactions of TMP-CFV and CFV-Time on Flux

The effects of two operating parameters (TMP and CFV) which also interact with time towards flux were drawn in form of three-dimensional plot. The purpose of this plotting is to convenience and comprehends the interaction between two operating conditions and also to locate their optimum levels.

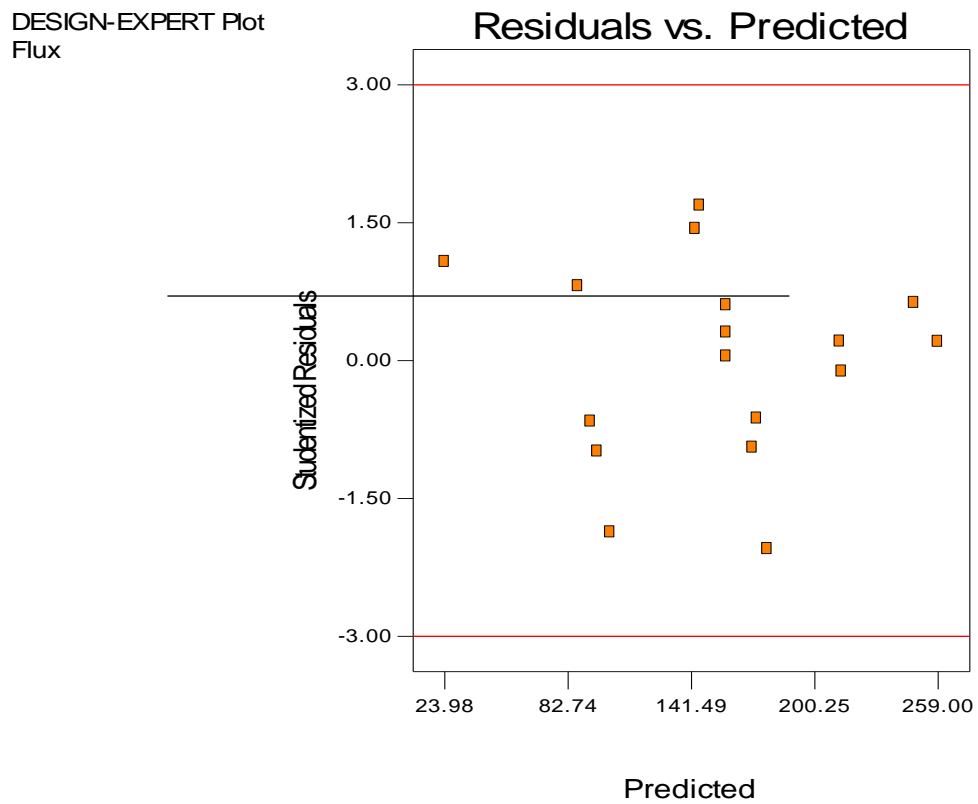
This model can be used to predict the flux within the limits of the experiment. The normal probability plot of the residuals, the plot of the residuals versus the predicted response and plot of outlier versus run for flux are shown in Figure 4.13-4.15. A check on the plot in Figure 4.13 revealed that the residuals generally fall on a straight line implying that errors are distributed normally, and thus, support adequacy of the least-square fit.

DESIGN-EXPERT Plot  
Flux



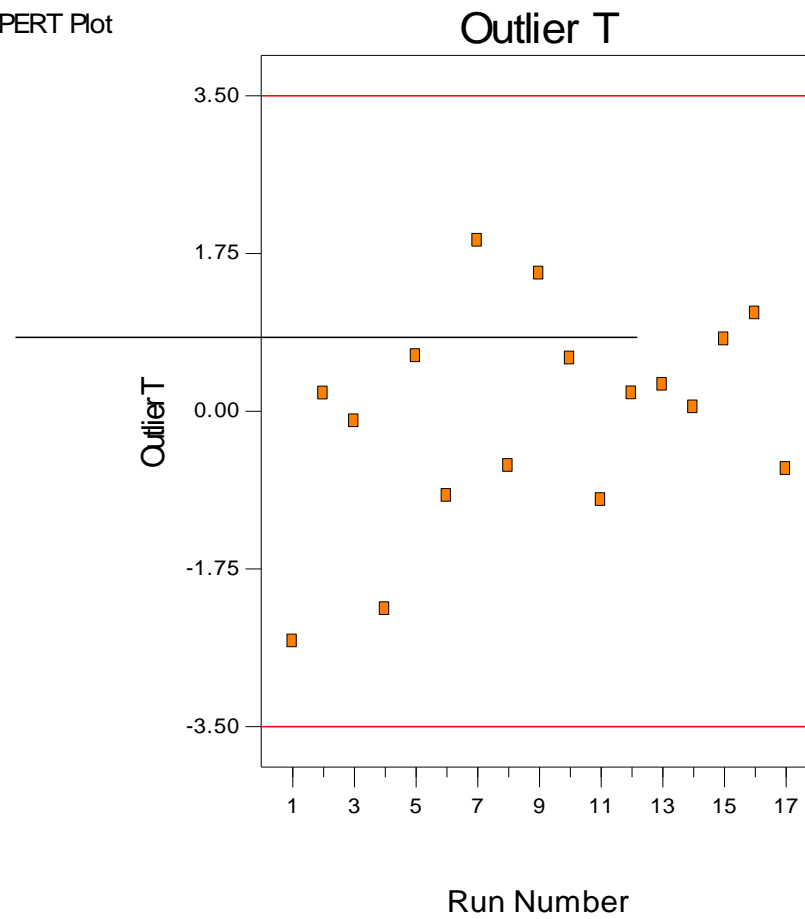
**Figure 4.13:** Normal probability plot of residual for flux.

Figure 4.14 and Figure 4.15 revealed that they have no obvious pattern and unusual structure. They also show equal scatter above and below the  $x$ -axis. This implies that the models proposed are adequate and there is no reason to suspect any violation of the independence or constant variance assumption.



**Figure 4.14:** Plot of residual vs. predicted response for flux.

DESIGN-EXPERT Plot  
Flux



**Figure 4.15:** Plot of outlier T vs. run for flux.

DESIGN-EXPERT Plot

Flux

X = A: TMP

Y = B: CFV

Actual Factor  
C: Time = 32.50

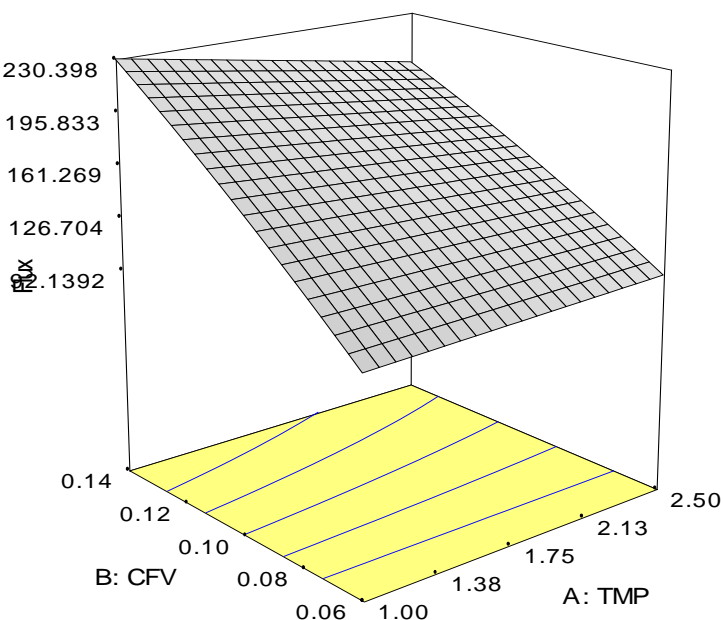


**Figure 4.16:** 3-D surface plot on flux for interaction of TMP (A) and CFV (B).

Figure 4.16 shows the response surface curves for the two variables in the permeate flux. The response surface representing the permeate flux was a function of one operating condition with the other one condition being at their optimal levels. Figure 4.16 revealed the operating conditions (TMP and CFV) gave the significant effect to the permeate flux. High value of CFV and TMP increased the permeate flux but the increases in TMP show a little improvement in permeate flux. Flux increases when the CFV changes from 0.06 to 0.14 m/s and TMP increases from 1.0 to 2.5 bars. The maximal permeate flux was obtained at 247.614 L/m<sup>2</sup>.h when the operating conditions was at TMP of 1.0 bar and CFV of 0.14 m/s within the duration of 20 minutes respectively.

## DESIGN-EXPERT Plot

Flux

X = B: CFV

Y = C: Time

Actual Factor

A: TMP = 1.75

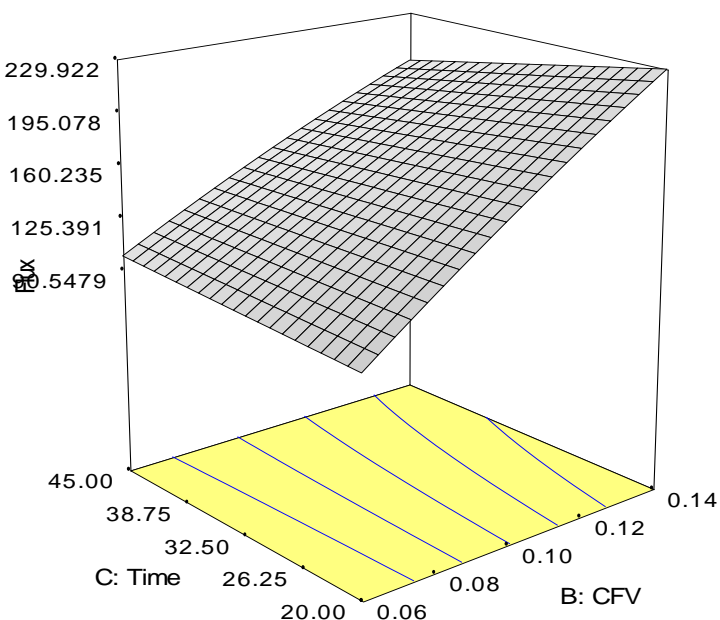


**Figure 4.17:** 3-D surface on flux rate for interaction of CFV (B) and Time (C).

Figure 4.17 shows the response surface curves for the interaction of CFV (B) and Time (C) on permeate flux. Figure 4.17 revealed the operating conditions (CFV and Time) gave the significant effect to the permeate flux. High value of CFV and Time increased the permeate flux but the increases in Time show a little increment in permeate flux. Flux increases when the CFV increases from 0.06 to 0.14 m/s and Time increases from 20 to 45 minutes. The maximal permeate flux was obtained at 247.614 L/m<sup>2</sup>.h when the operating conditions was at 1.0 bar of TMP and 0.14 m/s of CFV within the duration of 20 minutes respectively.

Based on research conducted by Catalayud *et al.*, (2010), result was shown on the effect of operating conditions on permeate flux and flux decline in the ultrafiltration of macromolecules. The statistical analysis results for average permeate flux illustrate that both the TMP and CFV have a remarkable influence on average flux. The result

obtained from this experiment was contradicted with the findings where higher TMP will increase the flux decline. However the permeate flux was increase as increase in TMP. Even though TMP give little effect on the permeate flux from this research, there is still little agreement where increase in TMP will increase the permeate flux. Besides that, the effect of CFV on permeate flux is similar with his findings where the increasing of CFV will results in increases of permeate flux. Furthermore higher flux decline was obtained with increases of CFV. Hence, the factor with the greatest influence on average flux is CFV followed by TMP (Catalayud *et al.*, 2010). As TMP rises, the average flux increases, but this increase is higher at higher values of CFV, which confirms the positive interaction.

## CHAPTER 5

### CONCLUSION AND RECOMMENDATION

#### 5.1 Conclusion

High value of cross flow velocity (CFV), transmembrane pressure (TMP) and Time increased the permeate flux but the increases in TMP and Time show a little increment in permeate flux. The maximal permeate flux obtained was at 247.614 L/m<sup>2</sup>.h when the operating conditions was at optimum TMP of 1.0 bar and CFV of 0.14 m/s within the duration of 20 minutes respectively. The combination between TMP and CFV enhance the permeate flux.

Effect of TMP and CFV on permeate flux were successfully been carried out throughout this research. The optimum TMP and CFV were achieved at 1.0 bar and 0.14 m/s respectively. Besides that, the objective of this research which to optimize the effect of TMP and CFV on permeate flux has also been achieved by using Response Surface Methodology.

## **5.2 Recommendation**

In order to enhance the separation process, appropriate pretreatment should be done on the membrane filter before performed the filtration process. The pretreatment can be performed after each experiment. Besides that, the material of construction of the membrane can be change from using ceramic membrane. Even the ceramic is resistance at high temperature and is strong in term of the structure; polyethersulfone (PES) membrane is more suitable for separation of carbohydrates. Apart from used the membrane with pore size of  $0.9\mu\text{m}$ , the smaller pore size of membrane should be used for example ultrafiltration membrane.

## REFERENCES

- Affleck, R. P. (2000). *Recovery of Xylitol from Fermentation of Model Hemicelluloses Hydrolysates Using Membrane Technology*. (Master's Thesis, Virginia Polytechnic Institute and State University, 2000). Retrieved from <http://scholar.lib.vt.edu/theses/available/etd-01102001-121200/unrestricted/turninetdII.pdf>.
- Ahmad, A. L., Ismail, S. and Bhatia, S. (2005). Membrane treatment for palm oil mill effluent: effect of transmembrane pressure and cross flow velocity. *Desalination*, 179: 245-255.
- Ahmad, A. L., Ibrahim, N. and Bowen, W. R. (2002). Automated electrophoretic membrane cleaning for dead-end microfiltration and ultrafiltration. *Separation and Purification Technology*, 29: 105-112.
- Alriols, M. G., Garcia, A., Llano-ponte, R. and Labidi, J. (2010). Combined organosolv and ultrafiltration lignocellulosic biorefinery process. *Chemical Engineering Journal*, 157: 113-120.
- Babel, S. and Takizawa, S. (2010). Microfiltration membrane fouling and cake behavior during algal filtration. *Desalination*, 261: 46-51.
- Batzias, F. A. and Sidiras, D. K. (2007). Simulation of dye adsorption by beech sawdust as affected by pH. *Journal of Hazardous Material*, 141: 668-679.

- Cara, C., Ruiz, E., Oliva, J. M., Saez, F. and Castro, E. (2008). Conversion of olive tree biomass into fermentable sugars by dilute acid pretreatment and enzymatic saccharification. *Bioresource Technology*, 99: 1869-1876.
- Catalayud, M. C. M., Vela, M. C. B., Blanco, S. A., Garcia, J. L. and Rodriguez, E. B. (2010). Analysis and optimization of the influence of operating conditions in the ultrafiltration of macromolecules using a response surface methodological approach. *Chemical Engineering Journal*, 156: 337-346.
- Choi, H., Zhang, K., Dionysiou, D. D., Oerther, D. B. and Sorial, G. A. (2005). Influence of cross-flow velocity on membrane performance during filtration of biological suspension. *Journal of Membrane Science*, 248: 189-199.
- Duarte, G. V., Ramarao, B. V. and Amidon, T. E. (2010). Polymer induced flocculation and separation of particulates from extracts of lignocellulosic materials. *Bioresource Technology*, 101: 8526-8534.
- Faria, L. F. F., Pereira, J. N. and Nobrega, R. (2002). Xylitol production from D-xylose in a membrane bioreactor. *Desalination*, 149: 231-236.
- Gonder, Z.B., Arayici S. and Barlas H. (2010). Advanced Treatment of Pulp and Paper Mill Wastewater by Nanofiltration Process: Effects of Operating Conditions on Membrane Fouling, *Separation and Purification Technology*, doi:10.1016/j.seppur.2010.10.018.
- Guo, G., Chen, W., Men, L. and Hwang, W. (2008). Characterization of dilute acid pretreatment of silver grass for ethanol production. *Bioresource Technology*, 99: 6046-6053.

- Gyura, J., Seres, Z. and Eszterle, M. (2005). Influence of operating parameters on separation of green syrup colored matter from sugar beet by ultra- and nanofiltration. *Journal of Food Engineering*, 66: 89-96.
- Hashino, M., Katagiri, T., Kubota, N., Ohmukai, Y., Maruyama, T. and Matsuyama, H. (2010). Effect of membrane surface morphology on membrane fouling with sodium alginate. *Journal of Membrane Science*. doi:10.1016/j.memsci.2010.10.014
- Hendriks, A. T. W. M. and Zeeman, G. (2009). Pretreatments to enhance the digestibility of lignocellulosic biomass. *Bioresource Technology*, 100: 10-18.
- Hu, G., Heitmann, J. A. and Rojas, O. J. (2008). Feedstock pretreatment strategies for producing ethanol from wood, bark, and forest residues. *Bioresources*, 3: 270-294.
- Huang, H. J., Ramaswamy, Shri., Tschirner, U. W. and Ramarao, B. V. (2008). A review of separation technologies in current and future biorefineries. *Separation and Purification Technology*, 62: 1-21.
- Hwang, K. J. and Sz, P. Y. (2009) Filtration characteristics and membrane fouling in cross- flow microfiltration of BSA/dextran binary Suspension. *Journal of Membrane Science*, 347: 75-82.
- Idris, A., Kormin, F. and Noordin, M. Y. (2006). Application of response surface methodology in describing the performance of thin film composite membrane. *Separation and Purification Technology*, 49: 271-280.
- Kumar, P., Barret, D. M., Delwiche, M. J. and Stroeve, Pieter. (2009). Methods for Pretreatment of Lignocellulosic Biomass for Efficient Hydrolysis and Biofuel Production. *Industrial. Engineering Chemical Resources*, 48: 3713-3729.

- Kumar, S., Singh, N. and Prasad, R. (2010). Anhydrous ethanol: A renewable source of energy. *Renewable and Sustainable Energy Reviews*, 14: 1830-1844.
- Lee, J. M., Shi, J., Venditti, R. A. and Jameel, H. (2009). Autohydrolysis pretreatment of Coastal Bermuda grass for increased enzyme hydrolysis. *Bioresource Technology*, 100: 6434-6441.
- Li, Y., Shahbazi, A. and Kadzere, C. T. (2006). Separation of cells and proteins from fermentation broth using ultrafiltration. *Journal of Food Engineering*, 75: 574-580.
- Liang, Y., Wang, Z., Ye, X., Li, W., Xi, X., Yang, L., Wang, X., Zhang, J., Liu, Y. and Cai, Z. (2010). Study on the control of pore sizes of membranes using chemical methods: Part III. The performance of carbonates and bicarbonates in the membrane-making process by the chemical reaction. *Desalination*, doi:10.1016/j.desal.2010.09.004
- Lin, S. H., Hung, C. L. and Juang, R. S. (2008). Effect of operating parameters on the separation of proteins in aqueous solutions by dead end ultrafiltration. *Desalination*, 234: 116-125.
- Madaeni, S. S. and Samieirad, S. (2010). Chemical cleaning of reverse osmosis membrane fouled by wastewater. *Desalination*, 257: 80-86.
- Mohammad, A. L. M. (2008). Recovery of hemicelluloses from wood hydrolysates by membrane filtration. (Master's Thesis, Lappeenranta University of Technology, 2000).
- Mosier, N., Wyman, C., Dale, B., Elander, R., Lee, Y. Y., Holtzapple, M. and Ladisch, M. (2005). Features of promising technologies for pretreatment of lignocellulosic biomass. *Bioresource Technology*, 96: 673-686.

- Puro, L., Kallioinen, M., Manttari, M., Natarajan, G., Cameron, D. C. and Nystrom, M. (2010). Performance of RC and PES ultrafiltration membranes in filtration of pulp mill process waters. *Desalination*, doi:10.1016/j.desal.2010.06.034
- Sakinah, A. M. M., Ismail, A. F., Ilyas, R. M. and Hassan, O. (2007). Fouling characteristics and autopsy of a PES ultrafiltration membrane in cyclodextrins separation. *Desalination*, 207: 227-242.
- Sakinah, A. M. M., Ismail, A. F., Illias, R. M., Zularisam, A. W., Hassan, O. and Matsuura, T. (2008). Cyclodextrin production in hollow fiber membrane reactor system: Effect of substrate preparation. *Separation and Purification Technology*, 63: 163-171.
- Sun, Y. and Cheng, J. (2002). Hydrolysis of lignocellulosic materials for ethanol production: a review. *Bioresource Technology*, 83: 1-11.
- Sun, Y. and Cheng, J. J. (2005). Dilute acid pretreatment of rye straw and bermudagrass for ethanol production. *Bioresource Technology*, 96: 1599-1606.
- Thomassen, J. K., Faraday, D. B. F., Underwood, B. O. and Cleaver, J. A. S. (2005). The effect of varying transmembrane pressure and cross flow velocity on the microfiltration fouling of a model beer. *Separation and Purification Technology*, 41: 91-100.
- Wang, Z., Keshwani, D. R., Redding, A. P. and Cheng, J. J. (2010). Sodium hydroxide pretreatment and enzymatic hydrolysis of coastal Bermuda grass. *Bioresource Technology*, 101: 3583-3585.
- Wikramasinghe, S. R. and Grzenia, D. L. (2008). Adsorptive membranes and resins for acetic acid removal from biomass hydrolysates. *Desalination*, 234: 144-151.

Zhong, Z., Xing, W., Liu, X., Jin, W. and Xu, N. (2007). Fouling and regeneration of ceramic membranes used in recovering titanium silicalite-1 catalysts. *Journal of Membrane Science*, 301: 67-75.

Zhu, J. Y. and Pan, X. J. (2010). Woody biomass pretreatment for cellulosic ethanol production: Technology and energy consumption evaluation. *Bioresource Technology*, 101: 4992-5002.

## APPENDIX A

### Preparation of Alkali and Acid solutions

#### A) 0.1M Sodium Hydroxide (NaOH)

$$n = MV/1000$$

$$\frac{m}{MW} = MV/1000$$

MW

where, n = mol

m = mass of NaOH needed

M = molarity @ concentration of NaOH = 0.1M

V = volume of solvent (H<sub>2</sub>O), mL = 100,000 mL

MW = molecular weight of NaOH, g/mol = 40 g/mol

Thus, 0.1M NaOH was prepared as follow:

$$\frac{m}{MW} = MV/1000$$

MW

$$m = ((0.1M)(100,000mL)/1000) \times 40 \text{ g/mol}$$

= **400 g of NaOH (solid)** needed to be diluting with 100 L distilled water  
to obtained 0.1M NaOH.

**B) 0.04M Sulfuric Acid (H<sub>2</sub>SO<sub>4</sub>)**

$$M = \frac{SG \times \text{purity} \times 1000}{MW}$$

where, M = molarity @ concentration of stock H<sub>2</sub>SO<sub>4</sub>

SG = specific gravity of H<sub>2</sub>SO<sub>4</sub> = 1.84

purity = percentage of stock H<sub>2</sub>SO<sub>4</sub> = 96% = 0.96

MW = molecular weight H<sub>2</sub>SO<sub>4</sub>, g/mol = 98.08 g/mol

Molarity of H<sub>2</sub>SO<sub>4</sub> needed from stock solution is as follow:

$$M = \frac{SG \times \text{purity} \times 1000}{MW} = \frac{1.84 \times 0.96 \times 1000}{98.08 \text{ g/mol}}$$

$$= 18.02 \text{ M}$$

Thus, using equation: M<sub>1</sub>V<sub>1</sub> = M<sub>2</sub>V<sub>2</sub>

$$(0.04\text{M})(100\text{L}) = (18.02\text{M})V_2$$

$$V_2 = 0.22 \text{ L}$$

= **220 mL stock H<sub>2</sub>SO<sub>4</sub>** is needed to be dilute  
with 100 L distilled water to obtained 0.04M  
H<sub>2</sub>SO<sub>4</sub>.

## APPENDIX B

### Calculation of permeate flux during separation process

Permeate flux was being calculated using following equation:

$$\begin{aligned} &\text{Permeate flux, } J \\ &= \frac{\text{permeate volume}}{\text{membrane area} \times \text{time}} (\text{L m}^{-2} \text{h}^{-1}) \quad \text{or} \quad J = \frac{Q}{A} \end{aligned}$$

where,  $J$  = permeate flux,  $\text{L/m}^2 \cdot \text{h}$

$Q$  = permeate flow rate,  $\text{mL/min}$

$A$  = effective membrane area,  $\text{m}^2 = 0.03\text{m}^2$

- A) Permeate flux at constant cross flow velocity (CFV = 0.06 m/s) at different values of transmembrane pressure (TMP).

Cross Flow Velocity, CFV = 0.06 m/s  
Transmembrane Pressure, TMP = 0.5 bar

Time (min)	Volume, V1 (mL)	Volume, V2 (mL)	Volume, Av (mL)	Flux (L/m <sup>2</sup> .h)
5	220	221	220.5	88.2
10	442	444	443	88.6
15	665	666	665.5	88.73333333
20	892	890	891	89.1
25	1118	1115	1116.5	89.32
30	1343	1342	1342.5	89.5
35	1563	1565	1564	89.37142857
40	1783	1784	1783.5	89.175
45	1998	2000	1999	88.84444444
50	2218	2220	2219	88.76
55	2440	2441	2440.5	88.74545455
60	2660	2662	2661	88.7

Cross Flow Velocity, CFV = 0.06 m/s  
Transmembrane Pressure, TMP = 1.0 bar

Time (min)	Volume, V1 (mL)	Volume, V2 (mL)	Volume, Av (mL)	Flux (L/m <sup>2</sup> .h)
5	215	250	232.5	93
10	440	500	470	94
15	660	745	702.5	93.66666667
20	870	995	932.5	93.25
25	1085	1230	1157.5	92.6
30	1297	1470	1383.5	92.23333333
35	1515	1710	1612.5	92.14285714
40	1730	1945	1837.5	91.875
45	1940	2180	2060	91.55555556
50	2156	2415	2285.5	91.42
55	2371	2650	2510.5	91.29090909
60	2587	2885	2736	91.2

Cross Flow Velocity, CFV = 0.06 m/s  
 Transmembrane Pressure, TMP = 1.5 bar

Time (min)	Volume, V1 (mL)	Volume, V2 (mL)	Volume, Av (mL)	Flux (L/m <sup>2</sup> .h)
5	240	245	242.5	97
10	490	495	492.5	98.5
15	705	730	717.5	95.66666667
20	965	965	965	96.5
25	1210	1205	1207.5	96.6
30	1455	1445	1450	96.66666667
35	1700	1690	1695	96.85714286
40	1950	1940	1945	97.25
45	2200	2185	2192.5	97.44444444
50	2450	2425	2437.5	97.5
55	2695	2670	2682.5	97.54545455
60	2940	2910	2925	97.5

Cross Flow Velocity, CFV = 0.06 m/s  
 Transmembrane Pressure, TMP = 2.0 bar

Time (min)	Volume, V1 (mL)	Volume, V2 (mL)	Volume, Av (mL)	Flux (L/m <sup>2</sup> .h)
5	225	225	225	90
10	445	460	452.5	90.5
15	670	700	685	91.33333333
20	895	935	915	91.5
25	1120	1175	1147.5	91.8
30	1345	1415	1380	92
35	1570	1650	1610	92
40	1800	1885	1842.5	92.125
45	2035	2125	2080	92.44444444
50	2260	2360	2310	92.4
55	2485	2600	2542.5	92.45454545
60	2710	2835	2772.5	92.41666667

Cross Flow Velocity, CFV = 0.06 m/s  
 Transmembrane Pressure, TMP = 2.0 bar

Time (min)	Volume, V1 (mL)	Volume, V2 (mL)	Volume, Av (mL)	Flux (L/m <sup>2</sup> .h)
5	210	235	222.5	89
10	420	475	447.5	89.5
15	645	720	682.5	91
20	865	955	910	91
25	1095	1190	1142.5	91.4
30	1325	1425	1375	91.66666667
35	1560	1660	1610	92
40	1785	1890	1837.5	91.875
45	2010	2120	2065	91.77777778
50	2220	2345	2282.5	91.3
55	2440	2570	2505	91.09090909
60	2665	2800	2732.5	91.08333333

- B) Permeate flux at constant transmembrane pressure (TMP = 1 bar) at different values of cross flow velocity (CFV).

Transmembrane Pressure, TMP = 1.0 bar

Cross Flow Velocity, CFV = 0.02 m/s

Time (min)	Volume, V1 (mL)	Volume, V2 (mL)	Volume, Av (mL)	Flux (L/m <sup>2</sup> .h)
5	45	45	45	18
10	85	95	90	18
15	123	140	131.5	17.53333333
20	161	185	173	17.3
25	199	230	214.5	17.16
30	239	275	257	17.13333333
35	274	320	297	16.97142857
40	310	362	336	16.8
45	348	405	376.5	16.73333333
50	386	448	417	16.68
55	424	492	458	16.65454545
60	462	537	499.5	16.65

Transmembrane Pressure, TMP = 1.0 bar

Cross Flow Velocity, CFV = 0.06 m/s

Time (min)	Volume, V1 (mL)	Volume, V2 (mL)	Volume, Av (mL)	Flux (L/m <sup>2</sup> .h)
5	215	250	232.5	93
10	440	500	470	94
15	660	745	702.5	93.66666667
20	870	995	932.5	93.25
25	1085	1230	1157.5	92.6
30	1297	1470	1383.5	92.23333333
35	1515	1710	1612.5	92.14285714
40	1730	1945	1837.5	91.875
45	1940	2180	2060	91.55555556
50	2156	2415	2285.5	91.42
55	2371	2650	2510.5	91.29090909
60	2587	2885	2736	91.2

Transmembrane Pressure, TMP = 1.0 bar

Cross Flow Velocity, CFV = 0.10 m/s

Time (min)	Volume, V1 (mL)	Volume, V2 (mL)	Volume, Av (mL)	Flux (L/m <sup>2</sup> .h)
5	405	380	392.5	157
10	825	760	792.5	158.5
15	1235	1145	1190	158.6666667
20	1647	1530	1588.5	158.85
25	2060	1910	1985	158.8
30	2475	2295	2385	159
35	2885	2670	2777.5	158.7142857
40	3295	3050	3172.5	158.625
45	3710	3435	3572.5	158.7777778
50	4120	3810	3965	158.6
55	4532	4190	4361	158.5818182
60	4944	4570	4757	158.5666667

Transmembrane Pressure, TMP = 1.0 bar

Cross Flow Velocity, CFV = 0.14 m/s

Time (min)	Volume, V1 (mL)	Volume, V2 (mL)	Volume, Av (mL)	Flux (L/m <sup>2</sup> .h)
5	640	630	635	254
10	1275	1245	1260	252
15	1915	1850	1882.5	251
20	2550	2475	2512.5	251.25
25	3190	2925	3057.5	244.6
30	3830	3325	3577.5	238.5
35	4470	3725	4097.5	234.1428571
40	5105	4125	4615	230.75
45	5740	4520	5130	228
50	6375	5000	5687.5	227.5
55	7010	5505	6257.5	227.5454545
60	7650	6010	6830	227.6666667

Transmembrane Pressure, TMP = 1.0 bar

Cross Flow Velocity, CFV = 0.18 m/s

Time (min)	Volume, V1 (mL)	Volume, V2 (mL)	Volume, Av (mL)	Flux (L/m <sup>2</sup> .h)
5	890	875	882.5	353
10	1780	1610	1695	339
15	2670	2400	2535	338
20	3560	3220	3390	339
25	4445	3975	4210	336.8
30	5335	4835	5085	339
35	6220	5605	5912.5	337.8571429
40	7110	6425	6767.5	338.375
45	8000	7210	7605	338
50	8885	8000	8442.5	337.7
55	9775	8800	9287.5	337.7272727
60	10660	9600	10130	337.6666667